

1 **REVIEW ARTICLE: THE USE OF REMOTELY PILOTED AIRCRAFT SYSTEMS**
2 **(RPAS) FOR NATURAL HAZARDS MONITORING AND MANAGEMENT**

3 Daniele Giordan¹, Yuichi Hayakawa², Francesco Nex³, Fabio Remondino⁴, Paolo Tarolli⁵

4 ¹Istituto di Ricerca per la Protezione Idrogeologica, Consiglio Nazionale delle Ricerche, Italy

5 ²Center for Spatial Information Science, The University of Tokyo, Japan

6 ³University of Twente, Faculty of Geo-Information Science and Earth Observation (ITC), The Netherlands

7 ⁴3D Optical Metrology (3DOM) Unit, Bruno Kessler Foundation (FBK), Trento, Italy

8 ⁵Department of Land, Environment, Agriculture and Forestry, University of Padova, Italy

9

10 **ABSTRACT**

11

12 The number of scientific studies that consider possible applications of Remotely Piloted Aircraft Systems
13 (RPAS) for the management of natural hazards effects and the identification of occurred damages are
14 strongly increased in last decade. Nowadays, in the scientific community, the use of these systems is not a
15 novelty, but a deeper analysis of literature shows a lack of codified complex methodologies that can be used
16 not only for scientific experiments but also for normal codified emergency operations. RPAS can acquire on-
17 demand ultra-high resolution images that can be used for the identification of active processes like landslides
18 or volcanic activities but also for the definition of effects of earthquakes, wildfires and floods. In this paper,
19 we present a review of published literature that describes experimental methodologies developed for the
20 study and monitoring of natural hazards.

21

22 **1. INTRODUCTION**

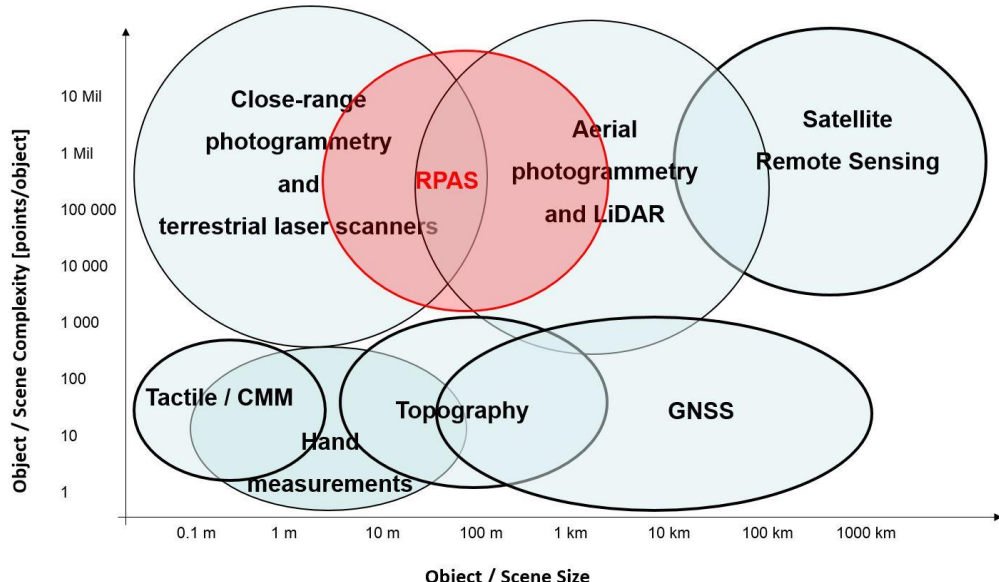
23

24 In last three decades, the number of natural disasters showed a positive trend with an increase in the number
25 of affected populations. Disasters not only affected the poor and characteristically more vulnerable countries
26 but also those thought to be better protected. Annual Disaster Statistical Review describes recent impacts of
27 natural disasters over population and reports 342 natural triggered disasters in 2016 (Guha-Sapir et al., 2017).
28 This is less than the annual average disaster frequency observed from 2006 to 2015 (376.4 events), however
29 natural disasters is still responsible for a high number of casualties (8,733 death). In the period 2006-2015,
30 the average number of casualties annaly caused by natural disasters is 69,827. In 2016, hydrological disasters
31 (177) had the largest share in natural disaster occurrence (51.8%), followed by meteorological disasters (96;
32 28.1%), climatological disasters (38; 11.1%) and geophysical disasters (31; 9.1%) (Guha-Sapir et al., 2017). To
33 face these disasters, one of the most important solutions is the use of systems able to provide an adequate
34 level of information for correctly understanding these events and their evolution. In this context, survey and
35 monitoring of natural hazards gained in importance. In particular, during the emergency phase it is very
36 important to evaluate and control the phenomenon evolution, preferably operating in near real time or real
37 time, and consequently, use this information for a better risk scenario assessment. The available acquired
38 data must be processed rapidly to ensure the emergency services and decision makers promptly.

39 Recently, the use of remote sensing (satellite and airborne platform) in the field of natural hazards and
40 disasters has become common, also supported by the increase in geospatial technologies and the ability to
41 provide and process up-to-date imagery (Joyce et al., 2009; Tarolli, 2014). Remotely sensed data play an
42 integral role in predicting hazard events such as floods and landslides, subsidence events and other ground
43 instabilities. Because their acquisition mode and capability for repetitive observations, the data acquired at
44 different dates and high spatial resolution can be considered as an effective complementary tool for field
45 techniques to derive information on landscape evolution and activity over wide areas.

46 In the context of remote sensing research, recent technological developments have increased in the field of
47 Remotely Piloted Aircraft Systems (RPAS) becoming more common and widespread in civil and commercial
48 context (Bendea et al., 2008). In particular, the development of photogrammetry and technologies associated
49 (i.e. integrated camera systems like compact cameras, industrial grade cameras, video cameras, single-lens
50 reflex (SLR) digital cameras and GNSS/INS systems) allow to use of RPAS platforms in various applications as
51 alternative to the traditional remote sensing method for topographic mapping or detailed 3D recording of
52 ground information and a valid complementary solution to terrestrial acquisitions too (Nex and Remondino,
53 2014) (Fig.1).

54 RPAS systems present some advantages in comparison to traditional platforms and, in particular, they could
55 be competitive thanks to their versatility in the flight execution (Gomez and Purdie, 2016). Mini/micro RPAS
56 are the most diffused for civil purposes, and they can fly at low altitudes according to limitations defined by
57 national aviation security agencies and be easily transported into the disaster area. Foldable Systems fits easily
58 into a daypack and can be transported safely as hand luggage. This advantage is particularly important for
59 first responder teams like UNDAC or similar. Stöcker et al. (2017) published a review of different state
60 regulations that are characterized by several differences regarding requirements, distance from the takeoff
61 and maximum altitude. Another important added value of RPAS is their adaptability that allows their use in
62 various typologies of missions, and in particular for monitoring operations in remote and dangerous areas
63 (Obanawa et al., 2014). The possibility to carry out flight operations at lower costs compared to ones required
64 by traditional aircraft is also a fundamental advantage. Limited operating costs make these systems also
65 convenient for multi-temporal applications where it is often necessary to acquire information on an active
66 process (like a landslide) over the time. A comparison between the use of satellite images, traditional aircraft
67 and RPAS has been presented and discussed by Fiorucci et al. (2018) for landslides applications and by
68 Giordan et al., (2017) for the identification of flooded areas. These comparisons show that RPAS are a good
69 solution for the on demand acquisition of high resolution images over limited areas.



70

71 Figure 1. Available geomatics techniques, sensors, and platforms for topographic mapping or detailed 3D
 72 recording of ground information, according to the scene dimensions and complexity (modified from Nex and
 73 Remondino, 2014).

74 RPASs are used in several fields as agriculture, forestry, archaeology and architecture, traffic monitoring,
 75 environment and emergency management. In particular, in the field of emergency assistance and
 76 management, RPAS platforms are used to reliably and fast collect data of inaccessible areas (Huang et al.,
 77 2017). Collected data can be mostly images but also gas concentrations or radioactivity levels as
 78 demonstrated by the tragic event in Fukushima (Sanada and Torii, 2015; Martin et al., 2016). Focusing on
 79 image collection, they can be used for early impact assessment, to inspect collapsed buildings and to evaluate
 80 structural damages on common infrastructures (Chou et al. 2010; Molina et al. 2012; Murphy et al., 2008;
 81 Pratt et al., 2009) or cultural heritage sites (Pollefeyts et al., 2001; Manfredini et al., 2012; Koutsoudisa et al.,
 82 2014; Lazzari et al., 2017). Environmental and geological monitoring can profit from fast multi-temporal
 83 acquisitions delivering high-resolution images (Thamm and Judex 2006; Niethammer et al. 2010). RPAS can
 84 be considered a good solution also for mapping and monitoring different active processes at the earth surface
 85 (Fonstad et al., 2013; Piras et al., 2017; Feurer et al., 2017; Hayakawa et al., 2018) such as: glaciers (Immerzel
 86 et al., 2014, Ryan et al., 2015; Fugazza et al., 2017), Antarctic moss beds (Lucieer et al., 2014b), costal areas
 87 (Delacourt et al., 2009; Klemas, 2015), Interseismic deformations (Deffontaines et al., 2017; 2018), river
 88 morphodynamic (Gomez and Purdie, 2016; Jaud et al., 2016; Aicardi et al., 2017; Bolognesi et al., 2016;
 89 Benassai et al., 2017), debri flows (Wen et al., 2011), and river channel vegetation (Dunford et al., 2009).

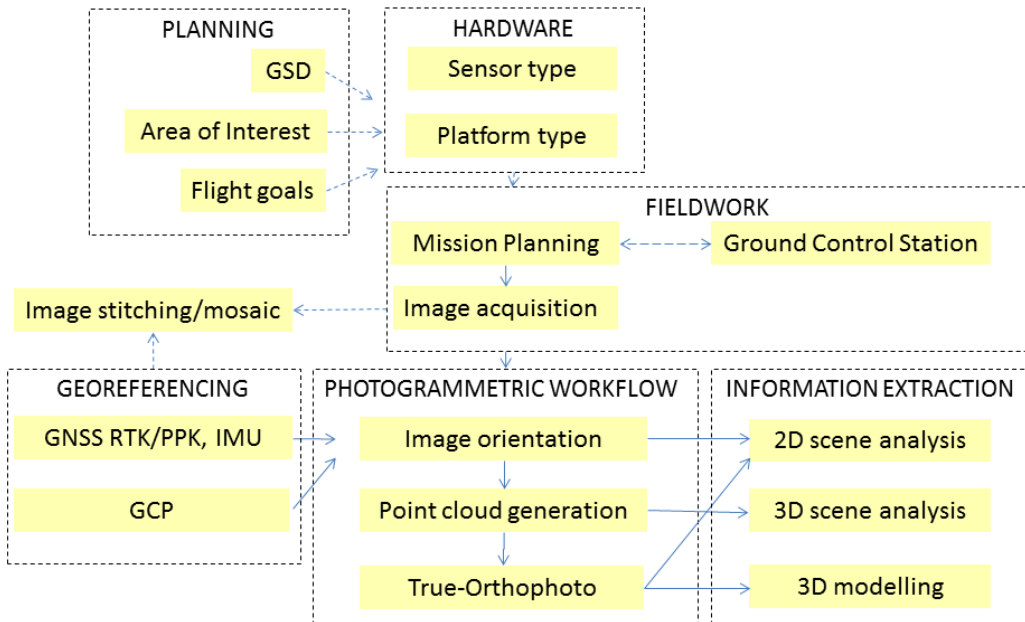
90 The incredible diffusion of RPAS has pushed many companies to develop dedicated sensors for these
 91 platforms. Besides the conventional RGB cameras other camera sensors are nowadays available on the
 92 market. Multi- and hyper-spectral cameras, as well as thermal sensors, have been miniaturized and
 93 customized to be hosted on many platforms.

94 The general workflow of a UAV acquisition is presented in Figure 2 below. The resolution of the images, the
 95 extension of the area as well as the goal of the flight are the main constraints that affect the selection of the
 96 platform and the typology of the sensor. Large areas can be flown using fixed wing (or hybrid) solutions able
 97 to acquire nadir images in a fast and efficient way. Small areas or complex objects (like steep slopes or
 98 buildings) should be acquired using rotor RPAS as they are usually slower but they allow the acquisition of
 99 oblique views. If the information different from the visible band is needed, the RPAS can host one or more

100 sensors acquiring in different bands. The flight mission can be planned using dedicated software: they range
101 from simple apps installed on smartphones in the low-cost solutions, to laptops connected to directional
102 antennas and remote controls for the most sophisticated platforms. According to the typology of the
103 platform, different GNSS and IMU can be installed. Low-cost solutions are usually able to give positions with
104 few meters accuracy and need GCP (Ground Control Points) to geo-reference the images. On the other hand,
105 most expensive solutions install double frequency GNSS receivers with the possibility to get accurate geo-
106 referencing thanks to Real Time Kinematic (RTK) or Post Processing Kinematic (PPK) corrections. The use of
107 GCP and different GNSS solutions is a fundamental point. Gercke and Przybilla (2016) presented the effect of
108 RTK-GNSS and cross flight patterns, and Nocerino et al., (2013) presented an evaluation about RPAS
109 processing results quality considering: i) the use of GCPs, ii) different photogrammetric procedures, iii)
110 different network configurations. If a quick mapping is needed, the information delivered by the navigation
111 system can be directly used to stitch the images and produce a rough image mosaicking (Chang-chun et al.,
112 2011). In the alternative, the typical photogrammetric process is followed: (i) image orientation, (ii) DSM
113 generation and (iii) orthophoto generation. The position (geo-referencing) and the attitude (rotation towards
114 the coordinates system) of each acquisition is obtained by estimating the image orientation. In the dense
115 point cloud generation, 3D point clouds are generated from a set of images, while the orthophoto is
116 generated in the last step combining the oriented images projected on the generated point cloud, leading to
117 orthorectified images (Turner et al., 2012). Point clouds can be very often converted in Digital Surface Models
118 (DSM), and Digital Terrain Models (DTM) can be extracted removing the off ground regions (mainly buildings
119 and trees). In real applications, many parameters can influenced the final resolution of DSM/DTM and
120 ortophoto like: real GSD (Nocerino et al., 2013) interior and exterior orientation parameters (Kraft et al.,
121 2016), overlap of images, flight strip configuration and used SfM-Software (Nex et al., 2015).

122 In particular during emergencies, the time required for the image dataset processing can be a critical point.
123 For this reason, the development of fast mosaicking methods as MACS, for a real time mapping applications
124 (Lehmann et al., 2011), or VABENE++, developed by German Aerospace Center for real time traffic
125 management (Detzer et al., 2015).

126 The outputs from the last two steps (point clouds and true-orthophotos) as well as the original images are
127 very often used as input in the scene understanding process: classification of the scene or extraction of
128 features (i.e. objects) of interest using machine learning techniques are the most common applications. 3D
129 models can also be generated using the point cloud and the oriented images to texturize the model.



130

131

Figure 2. Acquisition and processing of RPAS images: general workflow.

132 In this paper, the authors present an analysis and evaluation concerning the use of RPAS as alternative
 133 monitoring technique to the traditional methods, relating to the natural hazard scenarios. The main goal is
 134 to define and test the feasibility of a set of methodologies that can be used in the monitoring and mapping
 135 activities. The study is focused in particular on the use of mini and micro RPAS systems (Table 1). The
 136 following table listed the technical specifications of these two RPAS categories, again based on the current
 137 classification by UVS (Unmanned Vehicle Systems) International. Most of the mini or micro RPAS systems
 138 available integrate a flight control system, which autonomously stabilizes these platforms and enables the
 139 remotely controlled navigation. Additionally, they can integrate an autopilot, which allows an autonomous
 140 flight based on predefined waypoints. For the monitoring and mapping applications, mini- or micro RPAS
 141 systems are very useful as cost-efficient platforms for capturing real-time close-range imagery. These
 142 platforms can reach the area of investigation and take several photos and videos from several points and
 143 different angles of view (Gomez and Kato, 2014). For mapping applications, it is also possible to use this flight
 144 control data to geo-register the captured payload sensor data like still images or video streams (Eugster and
 145 Nebiker, 2008).

146 Table 1. Classification of mini and micro UAV systems, according to UVS International (UVS International,
 147 2018)

Category	Max. Take Off Weight	Max. Flight Altitude	Endurance	Data Link Range
Mini	<30kg	150-300m	<2h	<10km
Micro	<5Kg	250m	1h	<10km

148

149 2. USE OF RPAS FOR NATURAL HAZARDS DETECTION AND MONITORING 150

151 Gomez and Purdie (2016) published a detailed analysis of the use of RPAS for hazards and disaster risk
 152 monitoring. In our paper, we focused our attention on the most dangerous natural hazards that can be

153 analyzed using RPAS. According to the definitions used by Annual Disaster Statistical Review (Guha-Sapir et
154 al., 2017), the paper considers in particular: i) landslides, ii) floods iii) earthquakes v) volcanic activity vi)
155 wildfires. For each considered category of natural hazard, the paper presents a review of a large list of
156 published papers (171 papers), analyzing proposed methodologies and provided results, and underlining
157 strengths and limitations in the use of RPAS. The aims of this paper is the description of possible use of RPAS
158 in considered natural hazards, describing a general methodology for the use of these systems in different
159 contexts merging all previous published experiences.

160

161 2.1 Landslides

162 Landslides are one of the major natural hazards that produce each year enormous property damage
163 regarding both direct and indirect costs. Landslides are rock, earth or debris flows on slopes due to gravity.
164 The event can be triggered by a variety of external elements, such as intense rainfall, water level change,
165 storm waves or rapid stream erosion that cause a rapid increase in shear stress or decrease in shear strength
166 of slope-forming materials. Moreover, the pressures of increasing population and urbanization, human
167 activities such as deforestation or excavation of slopes for road cuts and building sites, etc., have become
168 important triggers for landslide occurrence. Because the factors affecting landslides can be geophysical or
169 human-made, they can occur in developed and undeveloped areas.

170 In the field of natural hazards, the use of RPAS for landslides study and monitoring represents one of the
171 most common applications. The number of papers that present case studies or possible methodologies
172 dedicated to this topic has strongly increased in last few years and now the available bibliography offers a
173 good representation of possible approaches and technical solutions.

174 When a landslide occurs, the first information to be provided is the extent of the area affected by the event
175 (figure 3). The landslide impact extent is usually done based on detailed optical images acquired after the
176 event. From these acquisitions, it is possible to derive Digital Elevation Models (DEMs) and orthophotos that
177 allow detecting main changes in geomorphological figures (Fan et al., 2017; Chang et al., 2017). In this
178 scenario, the use of the mini-micro RPAS is practical for small areas and optimal for landslides that often
179 cover an area that range from less than one square kilometres up to few square kilometres. Ultra-high
180 resolution images acquired by RPAS can support the definition not only of the identification of studied
181 landslide limit, but also the identification and mapping of main geomorphological features (Rossi et al., 2017;
182 Fiorucci et al., 2018). Furthermore, a sequence of RPAS acquisitions over the time can provide useful support
183 for the study of the gravitational process evolution.

184 According to Scaioni et al. (2014), applications of remote sensing for landslides investigations can be divided
185 into three classes: i) landside recognition, classification and post-event analysis, ii) landslide monitoring, iii)
186 landslide susceptibility and hazard assessment.

187



188

189 Figure 3. Example of RPAS image of a rockslide occurred on a road. The image was acquired after the
190 rockslide occurred in 2014 in San Germano municipality (Piemonte region, NW Italy). As presented in
191 Giordan et al. (2015a), a multi-rotor of local Civil Protection Agency was used to evaluate occurred damages
192 and residual risk. RPAS images can be very useful to have a representation from a different point of view of
193 the occurred phenomena. Even not already processed using SFM applications, this dataset can be very
194 useful for decision makers to define the strategy for the management of the first phase of emergency.

195

196 **2.1.1 Landslides recognition**

197 The identification and mapping of landslides are usually performed after intense meteorological events that
198 can activate or reactivate several gravitational phenomena. The identification and mapping of landslides can
199 be organized in landslides event maps. Landslides event mapping is a well-known activity obtained thought
200 field surveys (Santangelo et al., 2010), visual interpretation of aerial or satellite images (Brardinoni et al.,
201 2003; Ardizzone et al., 2013) combined analysis of LiDAR DTM and images (Van Den Eeckhaut et al., 2007;
202 Haneberg et al., 2008; Giordan et al., 2013; Razak et al., 2013; Niculită et al., 2016). The use of RPAS for the
203 identification and mapping of a landslide has been described by several authors (Niethammer et al 2009;
204 Niethammer et al 2010; Rau et al., 2011; Carvajal et al., 2011; Travelletti et al., 2012; Torrero et al., 2015;
205 Casagli et al., 2017). Niethammer et al 2009 and Liu et al. (2015) showed how RPAS could be considered a
206 good solution for the acquisition of ultra-high resolution images with low-cost systems. Fiorucci et al. (2018)
207 compared the results of the landslide limit mapped using different techniques and found that satellite images
208 can be considered a good solution for the identification and map of landslides over large areas. On the
209 contrary, if the target of the study is the definition of landslide's morphological features, the use of more
210 detailed RPAS images seemed to be the better solution. As suggested by Walter et al., (2009) and Huang et
211 al., (2017) one of the most critical elements for a correct georeferencing of acquired images are the use of
212 GCPs. The in situ installation and positioning acquisition of GCPs can be an important challenge in particular
213 in dangerous areas as active landslides. Very often, GCPs are not installed in the most active part of the slide

214 but on stable areas. This solution can be safer for the operator, but it can also reduce the accuracy of the
215 final reconstruction.

216 Another parameter that can be considered during the planning of the acquisition phase is the morphology of
217 the studied area. According to with Giordan et al., (2015b), slope materials and gradient can affect the flight
218 planning and the approach used for the acquisition of the RPAS images. Two possible scenarios can be
219 identified: i) steep to vertical areas ($>40^\circ$); ii) slopes with gentle to moderate slopes ($<40^\circ$). In the first case,
220 the use of multi-copters with oblique acquisitions is often the best solution. On the contrary, with more
221 gentle slopes, the use of fixed-wing systems can assure the acquisition of wider areas.

222

223 **2.1.2 Landslides monitoring**

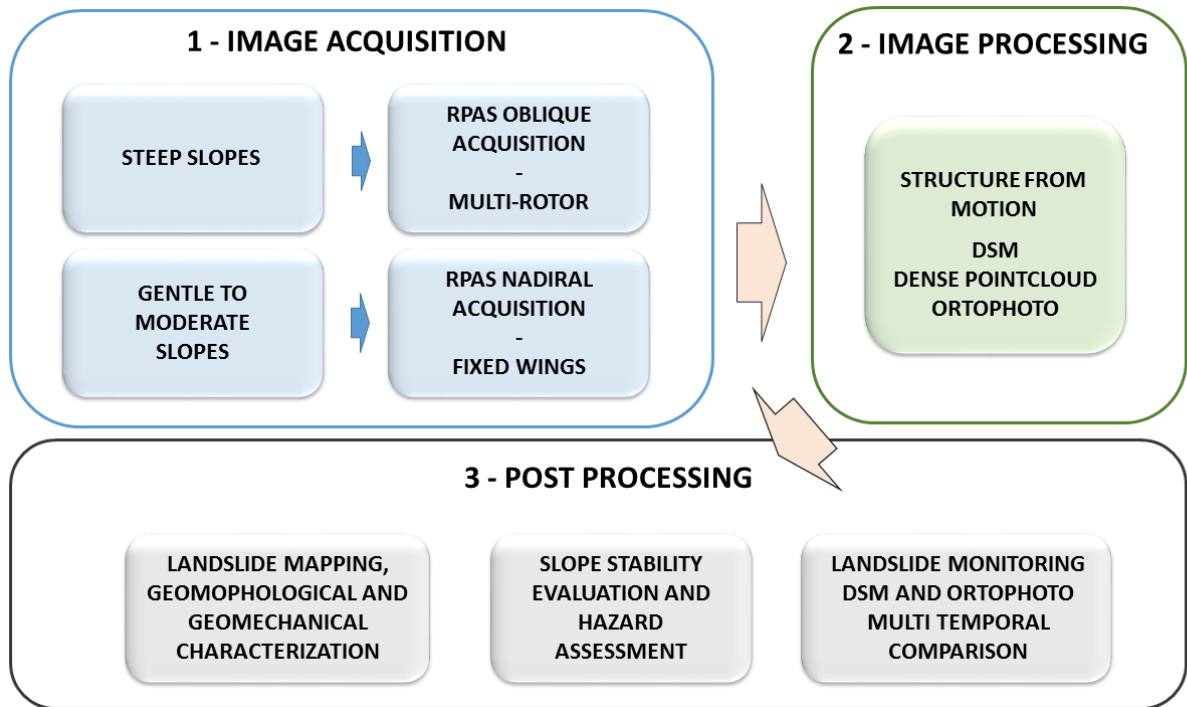
224 The second possible field of application of RPAS is the use of multi-temporal acquisitions for landslides
225 monitoring. This topic has been described by several authors (Dewitte et al., 2008; Turner and Lucieer, 2013;
226 Travelletti et al., 2012; Lucieer et al. 2014a; Turner et al., 2015; Marek et al., 2015; Lindner et al., 2016; Peppa
227 et al., 2017). In these works, numerous techniques based on the multi-temporal comparison of RPAS datasets
228 for the definition of the evolution of landslides have been presented and discussed. Niethammer et al. (2010
229 and 2012) described how the position change of geomorphological features (in particular fissures) could be
230 considered for a multi-temporal analysis with the aim of the characterization of the landslide evolution.
231 Travelletti et al. (2012) introduced the possibility of a semi-automatic image correlation to improve this
232 approach. The use of image correlation techniques has been also described by Lucieer et al. (2014a) who
233 demonstrated that COSI-Corr (Co-registration of Optically Sensed Imaged and Correlation - Leprince et al.
234 2007, 2008; Ayoub et al., 2009) can be adopted for the definition of the surface movement of the studied
235 landslide. A possible alternative solution is the multi-temporal analysis of the use of DSMs. The comparison
236 of digital surface models can be used for the definition of volumetric changes caused by the evolution of the
237 studied landslide. The acquisition of these digital models can be done with terrestrial laser scanners (Baldo
238 et al., 2009) or airborne LiDAR (Giordan et al., 2013). Westoby et al. (2012) emphasized the advantages of
239 RPAS concerning terrestrial laser scanner, which can suffer from line-of-sight issues, and airborne LiDAR,
240 which are often cost-prohibitive for individual landslide studies. Turner et al. (2015) stressed the importance
241 of a good co-registration of multi-temporal DSM for good results that could decrease the accuracy of results.
242 The use of benchmarks in areas not affected by morphological changes can be used for a correct calibration
243 of rotational and translation parameters.

244

245 **2.1.3 Landslides susceptibility and hazard assessment**

246 Landslides susceptibility and hazard assessment are often performed at basin scale (Guzzetti et al., 2005)
247 using different remote sensing techniques (Van Westen et al., 2008). The use of RPAS can be considered for
248 single case study applications to help decision makers in the identification of the landslide damages and the
249 definition of residual risk (Giordan et al., 2015a). Saroglou et al., (2017) presented the use of RPAS for the
250 definition of trajectories of rock falls prone areas. Salvini et al. (2017 and 2018) and Török et al., (2017)
251 described the combined use of TLS and RPAS for hazard assessment of steep rock walls. All these papers
252 considered the use of RPAS as a valid solution for the acquisition of DSM over sub-vertical areas. Török et al.,
253 (2017) and Tannant et al., 2017 also described in their manuscripts how RPAS DSMs can be used for the
254 evaluation of slope stability using numerical modelling. Fan et al. (2017) analyzed the geometrical features

255 and provided the disaster assessment of a landslide occurred on June 24 2017 in the village of Xinmo in
256 Maoxian County, (Sichuan Province, Southwest China). Aerial images were acquired the day after the event
257 from an unmanned aerial vehicle (UAV) (fixed-wing UAV, with a weight less than 10 kg, and flight autonomy
258 up to 4 hours), and a digital elevation model (DEM) was processed, with the purpose to analyzed the main
259 landslide geometrical features (front, rear edge elevation, accumulation area, horizontal sliding distance)



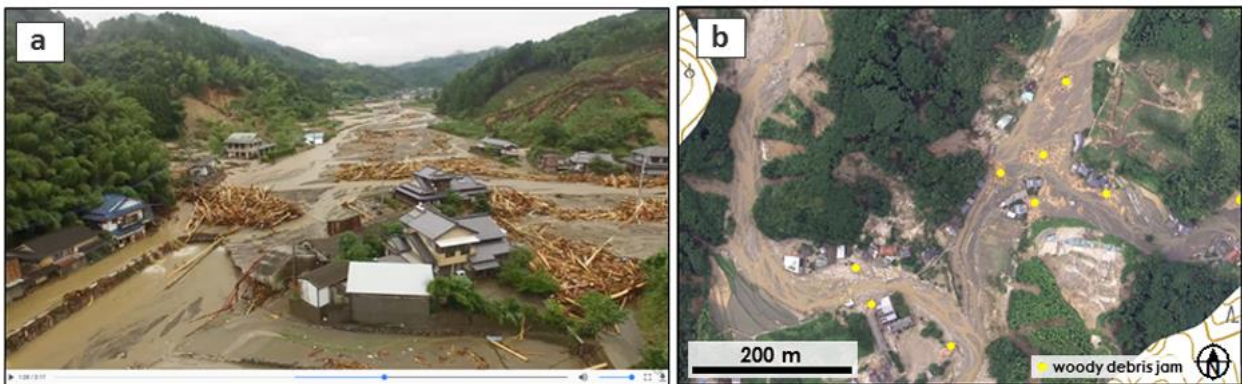
260

261
262 Figure 4. Acquisition, processing and post-processing of RPAS images applied to i) landslides recognition, ii)
263 hazard assessment and iii) slope evolution monitoring.

264

265 2.2 Floods

266 Disastrous floods in urban, lowland areas often cause fatalities and severe damage to the infrastructure.
267 Monitoring the flood flow, assessment of the flood inundation areas and related damages, post-flood
268 landscape changes, and pre-flood prediction are therefore seriously required. Among various scales of
269 approaches for flood hazards (Sohn et al., 2008), the RPAS has been adopted for each purpose of the flood
270 damage prevention and mitigation because it has an ability of quick measurement at a low cost (DeBell et
271 al., 2016; Nakamura et al., 2017). Figure 5 shows an example of the use of RPAS for prompt damage
272 assessment by a severe flood occurred on early July 2017 at northern Kyushu area, southwest Japan. The
273 Geospatial Information Authority of Japan (GSI) utilized an RPAS for the post-flood video recording and
274 photogrammetric mapping of the damaged area with flood flow and large woody debris.



275

276 Figure 5. Image captures of flood hazard using RPAS just after the 2017 Northern Kyushu Heavy Rain in the
 277 early July (southwest Japan), provided by GSI. (a) A screenshot of the aerial video of a flooded area along
 278 the Akatani River, Asakura City in Fukuoka Prefecture. (b) Orthorectified image of the damaged area.
 279 Locations of woody debris jam are mapped and shown on the online map (GSI, 2017). The video and map
 280 products are freely provided (compatible with Creative Commons Attribution 4.0 International).

281

282 **2.2.1. Potential analysis of flood inundation**

283 The risk assessments of flood inundation before the occurrence of a flood is crucial for the mitigation of the
 284 flood-disaster damages. RPAS is capable of providing quick and detailed analysis of the land surface
 285 information including topographic, land cover, and land use data, which are often incorporated into the
 286 hydrological modelling for the flood estimate (Costa et al., 2016). As a pre-flood assessment, Li et al. (2012)
 287 explored the area around an earthquake-derived barrier lake using an integrated approach of remote sensing
 288 including RPAS for the hydrological analysis of the potential dam-break flood. They proposed a technical
 289 framework for the real-time evacuation planning by accurately identifying the source water area of the
 290 dammed lake using a RPAS, followed by along-river hydrological computations of inundation potential.
 291 Tokarczyk et al. (2015) showed that the RPAS-derived imagery is useful for the rainfall-runoff modelling for
 292 the risk assessment of floods by mapping detailed land-use information. As a key input data, high-resolution
 293 imperviousness maps were generated for urban areas from RPAS imagery, which improved the hydrological
 294 modelling for the flood assessment. Zazo et al. (2015) and Šerban et al. (2016) demonstrated hydrological
 295 calculations of the potentially flood-prone areas using RPAS-derived 3D models. They utilized 2D cross
 296 profiles derived from the 3D model for the hydrological modelling.

297

298 **2.2.2. Flood monitoring**

299 Monitoring of the ongoing flood is potentially important for the real-time evacuation planning. Le Coz et al.
 300 (2016) mentioned that the movies captured by a RPAS, which can be operated by not only research specialists
 301 but also general non-specialists, is potentially useful for the quantitative monitoring of floods including flow
 302 velocity estimate and flood modelling. This can also contribute to the crowdsourced data collection for flood
 303 hydrology as the citizen science. In case of flood monitoring, however, areas under water is often problematic
 304 by image-based photogrammetry because the bed is not often fully seen in aerial images. If the water is clear
 305 enough, bed images under water can be captured, and the bed morphology can be measured with additional
 306 corrections of refraction (Tammenga et al., 2015; Woodget et al., 2015), but the flood water is often unclear
 307 because of the abundant suspended sediment and disturbing flow current. Another option is the fusion of

308 different datasets using a sonar-based measurement for the water-covered area, which is registered with
309 the terrestrial datasets (Flener et al., 2013; Javernick et al., 2014). Image-based topographic data of water
310 bottom by unmanned underwater vehicle (UUV, also known as an autonomous underwater vehicle, AUV)
311 can also be another option (e.g., Pyo et al., 2015), although such the application of UUV to flooding has been
312 limited.

313 Not only the use of topographic datasets derived from Structure from Motion-Multi Stereo View (SfM-MVS)
314 photogrammetry, the use of orthorectified images concurrently derived from the RPAS-based aerial images
315 is advantageous for the assessment of hydrological observation and modelling of floods. Witek et al. (2014)
316 developed an experimental system to monitor the stream flow in real time for the prediction of overbank
317 flood inundation. The real-time prediction results are also visualized online with a web map service with a
318 high-resolution image (3 cm/pix). Feng et al. (2015) reported that the accurate identification of inundated
319 areas is feasible using RPAS-derived images. In their case, deep learning approaches of the image
320 classification using optical images and texture by RPAS successfully extracted the inundated areas, which
321 must be useful for flood monitoring. Erdelj et al. (2017) proposed a system that incorporates multiple RPAS
322 devices with wireless sensor networks to perform the real-time assessment of a flood disaster. They
323 discussed the technical strategies for the real-time flood disaster management including the detection,
324 localization, segmentation, and size evaluation of flooded areas from RPAS-derived aerial images.

325

326 **2.2.3. Post-flood changes**

327 Post-flood assessments of the land surface materials including topography, sediment, and vegetation are
328 more feasible by RPAS surveys (Izumida et al., 2017). Smith et al. (2014) proposed a methodological
329 framework for the immediate assessment of flood magnitude and affected landforms by SfM-MVS
330 photogrammetry using both aerial and ground-based photographs. In this case, it is recommended to
331 carefully select appropriate platforms for SfM-MVS photogrammetry (either airborne or ground-based)
332 based on the field conditions. Tamminga et al. (2015) examined the 3D changes in river morphology by an
333 extreme flood event, revealing that the changes in reach-scale channel patterns of erosion and deposition
334 are poorly modelled by the 2D hydrodynamics based on the initial condition before the flood. They also
335 demonstrate that the topographic condition can be more stable after such an extreme flood event.
336 Langhammer et al. (2017) proposed a method to quantitatively evaluate the grain size distribution using
337 optical images taken by a RPAS, which is applied to the sediment structure before and after a flash flood.

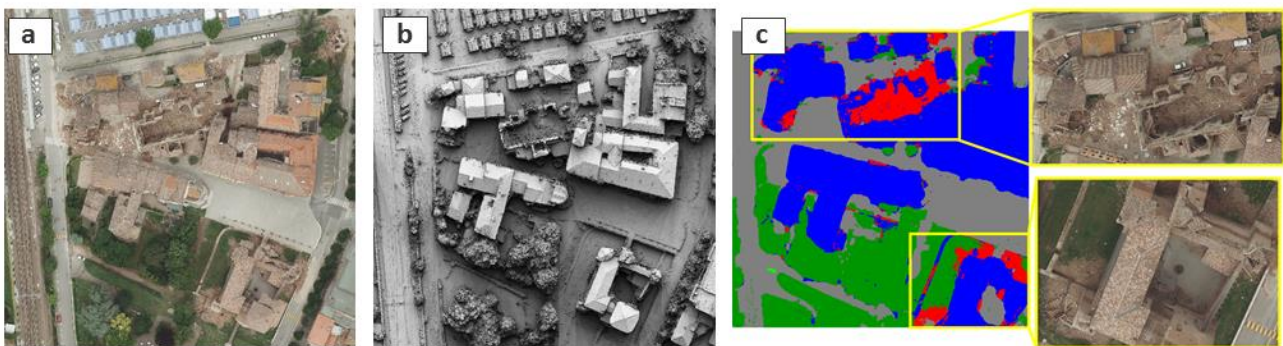
338 As a relatively long-term study, Dunford et al. (2009) and Hervouet et al. (2011) explored annual landscape
339 changes after the flood using RPAS-derived images together with other datasets such as satellite image
340 archives or a manned motor paraglider. Their work assessed the progressive development of vegetation on
341 a braided channel at an annual scale, which appears to be controlled by local climate including rainfall,
342 humidity, and air temperature, hydrology, groundwater level, topography, and seed availability. Changes in
343 the sediment characteristics by a flood is another key feature to be examined.

344

345 **2.3 Earthquakes**

346 Remote sensing technology has been recognized as a suitable source to provide timely data for automated
347 detection of damaged buildings for large areas (Dong and Shan, 2013; Pham et al., 2014; Cannioto et al.,
348 2017). In the post-event, satellite images have been traditionally used for decades to visually detect the

349 damages on the buildings to prioritize the interventions of rescuers. Operators search for externally visible
350 damage evidence such as spalling, debris, rubble piles and broken elements, which represent strong
351 indicators of severe structural damage. Several researches, however, have demonstrated how this kind of
352 data often leads to the wrong detection, usually underestimating the number of the collapsed building
353 because of their reduced resolution on the ground. In this regard, airborne images and in particular oblique
354 acquisitions (Tu et al., 2017; Nex et al., 2014; Gerke and Kerle 2011; Nedjati et al., 2016) have demonstrated
355 to be a better input for reliable assessments, allowing the development of automated algorithms for this task
356 (Figure 6). The deployment of photogrammetric aeroplanes on the strike area is however very often
357 unfeasible especially when the early (in the immediate hours after the event) damage assessment for
358 response action is needed.



359

360 Figure 6. True-orthophoto, Digital Surface Model and damage map of an urban area using airborne nadir
361 images (Source: Nex et al., 2014).

362 For this reason, RPASs have turned out to be valuable instruments for the building damage assessment
363 (Hirose et al., 2015). The main advantages of RPASs are their availability (and reduced cost) and the ease to
364 repeatedly acquire high-resolution images. Thanks to their high resolution, their use is not only limited to the
365 early impact assessment for supporting rescue operations, but it is also considered in the preliminary analysis
366 of the structural damage assessment.

367

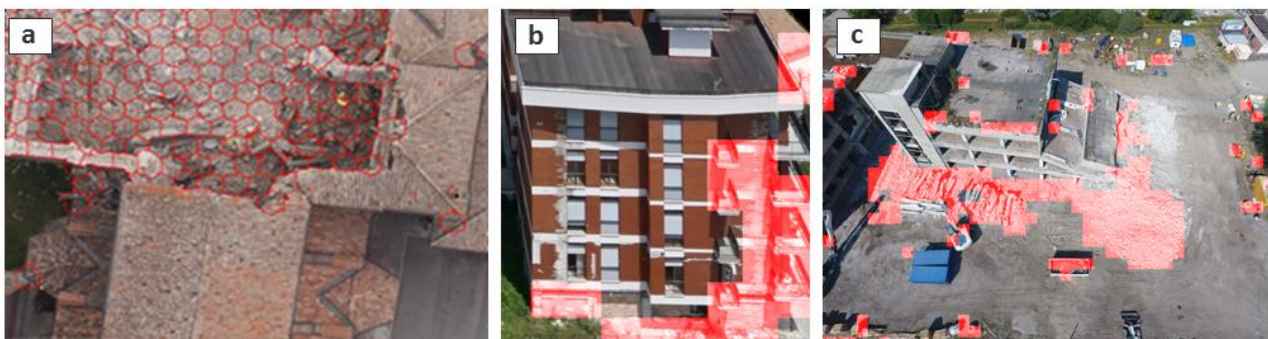
368 **2.3.1 Early impact assessment**

369 The fast deployment in the field, the easiness of use and the capability to provide in real time high-resolution
370 information of inaccessible areas to prioritize the operator's activities are the strongest point of RPASs for
371 these activities (Boccardo et al., 2015). The use of RPASs for rescue operations started almost a decade ago
372 (Bendea et al., 2008) but their massive adoption has begun only in the very last few years (Earthquake in
373 Nepal 2015) thanks to the development of low cost and easy to use platforms. Initiatives like *UAViators*
374 (<http://uaviators.org/>) have further increased the public awareness and acceptance of this kind of
375 instruments. Several rescue departments have now introduced RPAS as part of the conventional equipment
376 of their teams (Xie et al., 2014). The huge number of videos acquired by RPAS and posted by rescuers online
377 (i.e. Youtube) after the 2016 Italian earthquakes confirm this general trend.

378 The operators use RPASs to fly over the interest area and get information through visual assessment of the
379 streaming videos. The quality of this analysis is therefore limited to the ability of the operator to fly the RPAS
380 over the interest area. The lack of video geo-referencing usually reduces the interpretability of the scene and
381 the accurate localization of the collapsed parts: only small regions can be acquired in a single flight. The lack

382 of georeferenced maps prevents the smooth sharing of the collected information with other rescue teams
383 limiting the practical exploitation of these instruments. RPASs are mainly used in daylight conditions as the
384 flight during the night is extremely critical, and the use of thermal images is of limited help for the rescuers.

385 Many researchers have developed algorithms to automatically extract damage information from imagery
386 (Figure 7). The main focus of these works is to reliably detect damages in a reduced time to satisfy the time
387 constraints of the rescuers. In (Vetrivel et al., 2015) the combined use of images and photogrammetric point
388 clouds have shown promising results thanks to a supervised approach. This work, however, highlighted how
389 the classifier and the designed 2D and 3D features were hardly transferable to different datasets: each scene
390 needed to be trained independently strongly limiting the efficiency of this approach. In this regard, the recent
391 developments in machine learning (i.e. Convolutional Neural Networks, CNN) have overcome these limits
392 (Vetrivel et al., in press), showing how they can correctly classify scenes even if they were trained using other
393 datasets: a trained classifier can be directly used by rescuers on the acquired images without need for further
394 operations. The drawback of these techniques is the computational time: the use of CNN, processing like
395 image segmentation or point cloud generation are computationally demanding and hardly compatible with
396 real-time needs. In this regard, most recent solutions exploit only images (i.e. no need to generate point
397 cloud) and limit the use of most expensive processes to the regions where faster classification approaches
398 provide uncertain results to deliver an almost real-time information (Duarte et al., 2017).



399

400 Figure 7. Examples of damage detection on images acquired in three different scenarios (a) Mirabello (source: Vetrivel
401 et al., in press) and (b) L'Aquila and Lyon (source Duarte et al., 2017).

402

403 2.3.2 Building damage assessment

404 The damage evidence that can be captured from a UAV is not sufficient to infer the actual damage state of
405 the building as it requires additional information such as damages to internal building elements (e.g., columns
406 and beams) that cannot be directly defined from images. Even though this information is limited, images can
407 provide useful information about the external condition of the structure, evidencing anomalies and damages
408 and providing a first important information for structural engineers. Two main typologies of investigations
409 can be performed: (i) the use of images for the detection of cracks or damages on the external surfaces of
410 the building (i.e. walls and roofs) and (ii) the use of point clouds (generated by photogrammetric approach)
411 to detect structural anomalies like tilted or deformed surfaces. In both cases, the automated processing can
412 only support and ease the work of the expert who still interprets and assess the structural integrity of the
413 building.

414 In (Fernandez-Galarreta et al., 2015) a comprehensive analysis of both point clouds and images to support
415 the ambiguous classification of damages and their use for damage score was presented. In this paper, the
416 use of point clouds was considered efficient for more serious damages (partial or complete collapse of the
417 building), while images were used to identify smaller damages like cracks that can be used as the basis for
418 the structural engineering analysis. The use of point clouds is investigated in (Baiocchi et al., 2013; Dominici
419 et al., 2017): this contribution highlights how point clouds from UAVs can provide very useful information to
420 detect asymmetries and small deformations of the structure.

421

422 2.4 Volcanic activity

423

424 RPAS is particularly advantageous when the target area of measurement is hardly accessible on the ground
425 due to dangers of volcanic gas or risks of eruption in volcanic areas (Andrews, 2015). Although an equipment
426 of RPAS can be lost or damaged by the volcanic activities, the operator can safely stay in a remote place.
427 Various sensors can be mounted on a RPAS to monitor volcanic activities including topography, land cover,
428 heat, gas composition, and even gravity field (Saiki and Ohba, 2010; Deurloo et al., 2012; Astuti et al., 2009;
429 Middlemiss et al., 2016). The photogrammetric approach to obtain topographic data is widely applied
430 because RGB camera sensors are small enough to be mounted on a small aircraft. As mentioned before, this
431 paper considers in particular small RPAS. In the study of volcanoes, larger aircrafts with a payload of kilograms
432 are also utilized to mount other types of sensors to monitor various aspects of their dynamic activities. For
433 this reason, in this chapter we consider also larger RPAS solutions.

434

435 2.4.1. Topographic measurements of volcanoes

436 Long-distance flight of a RPAS enables quick and safe measurements of an emerging volcanic island. Tobita
437 et al. (2014a) successfully performed a fixed-wing RPAS flight for a one-way distance of 130 km in total flight
438 time of 2 hours and 51 minutes over the sea to capture aerial images of a newly formed volcanic island next
439 to Nishinoshima Island (Ogasawara Islands, southwest Pacific). They performed SfM-MVS photogrammetry
440 of the aerial images taken back from the RPAS to generate a 2.5 m resolution DEM of the island. The team
441 also performed two successive measurements of Nishinoshima Island in the following 104 days, revealing the
442 morphological changes in the new island covering a 1,600 m by 1,400 m area (Nakano et al., 2014; Tobita et
443 al., 2014b).

444 Since the volcanic activities often last for a long period, it is also important to connect the recent volcanic
445 morphological changes to those in the past. Although detailed morphological data of volcanic topography is
446 often unavailable, historical aerial photographs taken in the past decades can be utilized to generate
447 topographic models at a certain resolution. Some case studies have used archival aerial photographs in
448 volcanoes for periods of more than 60 years, generating DEMs with resolutions of several meters for areas
449 of 10 km² (Gomez, 2014; Derrien et al., 2015; Gomez et al. 2015). Although these DEMs are coarser than
450 those derived from RPAS, they can be used as supportive datasets for the modern morphological monitoring
451 using RPAS at a higher resolution and measurement frequency.

452

453 2.4.2. Gas monitoring and product sampling

454 Caltabiano et al. (2005) proposed the architecture of a RPAS for the direct monitoring of gas composition in
455 volcanic clouds of Mt. Etna in Italy. In this system, the 2-m wide fixed-wing RPAS can fly autonomously up to
456 4000 m altitude with a speed of 40 km/h. Like this system, a RPAS with a payload of several kilograms can
457 carry multiple sensors to monitor different compositions of volcanic gas. McGonigle et al. (2008) used a RPAS
458 for volcanic gas measurements at La Fossa crater of Mt. Vulcano in Italy. The RPAS has 3 kg payload and
459 allows to host an ultraviolet spectrometer, an infrared spectrometer, and an electrochemical sensor on
460 board. The combination of these sensors enabled the estimation of the flux of SO₂ and CO₂, which are crucial
461 for revealing the geochemical condition of erupting volcanoes. The monitoring of gas composition including
462 CO₂, SO₂, H₂S, H₂, as well as the air temperature, can be used for the quantification of the degassing activities
463 and prediction of the conduit magma convection, as suggested by the tests at several volcanoes in Japan
464 (Shinohara, 2013; Mori et al., 2014) and in Costa Rica (Diaz et al., 2015).

465 A RPAS can also transport a small ground-running robot (Unmanned Ground Vehicle: UGV) to slope head of
466 an active volcano, where the UGV takes close-range photographs of volcanic ash on the ground surface by
467 running down the slope (Nagatani et al., 2013). Protocols for direct sampling of volcanic products using a
468 RPAS have also been developed (Yajima et al., 2014).

469

470 **2.4.3. Geothermal monitoring**

471 In New Zealand, Harvey et al. (2016) and Nishar et al. (2016) carried out experimental studies on the regular
472 monitoring of intense geothermal environments using a small RPAS. They used thermal images taken by an
473 infrared imaging sensor together with normal RGB images for photogrammetry, mapping both the ground
474 surface temperature with detailed topography and land cover data. Chio and Lin (2017) further assessed the
475 use of a RPAS equipped with a thermal infrared sensor for the high-resolution geothermal image mapping in
476 a volcanic area in Taiwan. They improved the measurement accuracies using an onboard sensor capable of
477 post-processed kinematic GNSS positioning. This allows accurate mapping with less ground control points,
478 which are hard to place on such intense geothermal fields.

479

480 **2.5 Wildfires**

481 Wildfires are a phenomenon with local and global effects (Filizzola et al., 2017). Wildfires represent a serious
482 threat for land managers and property owners; in the last few years, this threat has significantly expanded
483 (Peters et al., 2013). The literature also suggests that climate change will continue to enhance the potential
484 forest fire activity in different regions of the world (McKenzie et al. 2014; Abatzoglou and Williams, 2016).
485 Remote sensing technologies can be very useful in monitoring such hazard (Shroeder et al., 2016). Several
486 scientists in the last few years used satellites in fire monitoring (Shroeder et al., 2016). More recently, RPASs
487 have been considered to be useful as well (Martinez-de Dios et al., 2011). Hinkley and Zajkowski (2011)
488 presented the results of a collaborative partnership between NASA, and the US Forest Service established
489 for testing thermal image data for wildfires monitoring. A small unmanned airborne system served as a sensor
490 platform. The outcome was an improved tool for wildfire decision support systems. Merino et al. (2012)
491 described a system for forest fire monitoring using a RPAS. The system integrates the information from the
492 fleet of different vehicles to estimate the evolution of the forest fire in real time. The field tests indicated
493 that RPAS could be very helpful for the activities of firefighting (e.g. monitoring). Indeed, they cover the gap
494 between the spatial scales given by satellites and those based on cameras. Wing et al. (2014) underlined the
495 fact that spectral and thermal sensors mounted in RPASs may hold great promise for future remote sensing

496 applications related to forest fires. RPASs have greater potential to provide enhanced flexibility for
497 positioning and repeated data collection. Tang and Shao (2015) summarize various approaches of remote
498 drone sensing to surveying forests, mapping canopy gaps, measuring forest canopy height, tracking forest
499 wildfires, and supporting intensive forest management. These authors underlined the usefulness in using
500 drones for wildfire monitoring. RPASs can repeatedly fly to record the extent of an ongoing wildfire without
501 jeopardizing crews' safety. Zajkowski et al. (2015) tested different RPASs (e.g. quadcopter, fixed-wing) for the
502 analysis of fire activity. Measurements included visible and long-wave infrared (LWIR) imagery, black carbon,
503 air temperature, relative humidity and three-dimensional wind speed and direction. The authors also
504 described in detail the mission's plan, including the logistics of integrating RPAS into a complex operations
505 environment, specifications of the aircraft and their measurements, execution of the missions and
506 considerations for future missions. Allison et al. (2016) provided a detailed state of the art on fire detection
507 using both manned and unmanned aerial platforms. This review highlighted the following challenges: the
508 need to development of robust automatic detection algorithms, the integration of sensors of varying
509 capabilities and modalities, the development of best practices for the use of new sensor platforms (e.g. mini
510 RPAS), and their safe and effective operation in the airspace around a fire.

511

512 **3. Discussion and conclusion**

513 In this paper, we analysed possible applications of RPAS to natural hazards. The available literature on this
514 topic is strongly increased in last few years, according to the improvement of the diffusion of these systems.
515 In particular, we considered: landslides, floods, earthquakes, volcanic activities and wildfires.

516 RPAS can support studies on active geological processes and can be considered a good solution for the
517 identification of effects and damages due to several catastrophic events. One of the most important elements
518 that characterized the use of RPAS is their flexibility and versatility, largely confirmed by the wide number of
519 operative solutions available in the literature. The available literature pointed out the necessity of the
520 development of dedicated methodologies that can be able to take the full advantage of RPAS. In particular,
521 typical results of structure from motion software (orthophoto and DSM) that are considered the end of
522 standard data-processing, can be very often the starting point of dedicated procedures specifically conceived
523 for natural hazards applications.

524 In the pre-emergency phase, one of the main advantages of RPAS surveys is to acquire high resolution and
525 low-cost data to analyse and interpret environmental characteristics and potential triggering factors (e.g.
526 slope, lithology, geostructure, land use/land cover, rock anomalies, and displacement). The data can be
527 collected with high revisit times to obtain multi-temporal observations. After the characterization of hazard
528 potential and vulnerability, some areas can be identified by a higher level of risk. These cases request an
529 intensive monitoring, to gain a quantitative evaluation of the potential occurrence of an event. In this
530 context, the use of aerial data represents a very useful complementary data source concerning the
531 information acquired through ground-based observations in particular for dangerous areas.

532 During the emergency phase, high-resolution imagery is asked to be acquired over the event site. The primary
533 use of this data is for the assessment of the damage grade (extent, type and damage grades specific to the
534 event and eventually of its evolution). They may also provide relevant information that is specific to critical
535 infrastructures, transport systems, aid and reconstruction logistics, government and community buildings,
536 hazard exposure, displaced population, etc (Ezequiel et al., 2014). Concurrently, the availability of clear and
537 straightforward raster and vector data, integrated with base cartographic contents (transportation, surface

538 hydrology, boundaries, etc.) it is recognized as an added-value to support decision makers for the
539 management of emergency operations (Fikar et al., 2016). These applications very often need prompt and
540 reliable interventions. RPAS should, therefore, deliver information promptly. In this regard, very few
541 researchers have focused on this issue: most of the reported works present (often time-consuming and even
542 manual) post-processing of the acquired data, precluding the use of their results from practical and real-life
543 scenarios. A big effort should be taken by the research community to propose faster and automated
544 approaches. In particular during emergencies, the time required for RPAS dataset processing is an important
545 element that should be carefully considered. Giordan et al. (2015a) presented a case study related to a
546 landslide emergency. In this paper, authors considered not only possible results but also the time that is
547 required for them

548 As in many other domains, RPAS present a disruptive technology where, beside conventional SfM
549 applications for 3D reconstructions, many dedicated and advanced methodologies are still in their
550 experimental phase and will need to be further developed in the incoming years. In the following years, it
551 would be desirable to witness the transfer of the best practices in the use of RPAS be then from the Research
552 community to Government Agencies (or private companies) involved in the prevention and reduction of
553 impacts of natural hazards. The Scientific community should contribute to the definition of standard
554 methodologies that can be assumed by civil protection agencies for the management of emergencies.

555 **References**

556 Abatzoglou, J.T. and Williams, A.P.: Impact of anthropogenic climate change on wildfire across western US
557 forests, *PNAS*, 113 (42), 11770-11775, 2016.

558 Astuti, \G., Giudice, G., Longo, D., Melita, C. D., Muscato, G. and Orlando, A.: An overview of the “Volcan
559 project”: An UAS for Exploration of volcanic environments, *J Intell. Robot Syst.*, 54, 471-494, 2009.

560 Aicardi, I., Chiabrando, F., Lingua, A., Noardo, F., Piras, M. and Vigna, B.: A methodology for acquisition and
561 processing of thermal data acquired by UAVs: a test about subfluvial springs’ investigations, *Geomatics,*
562 *Natural Hazards and Risk.* 8:1, 5-17, 2017. DOI: 10.1080/19475705.2016.1225229

563 Allison R.S., Johnston J.M., Craig G. and Jennings S.: Airborne Optical and Thermal Remote Sensing for
564 Wildfire Detection and Monitoring Sensors, 16(8), 1310, doi:10.3390/s16081310, 2016

565 Andrews, C.: Pressure in the danger zone [volcanoes], *Eng. Technol.*, 10(7), 56–61, doi:10.1049/et.2015.0720,
566 2015.

567 Ardizzone, F., Fiorucci, F., Santangelo, M., Cardinali, M., Mondini, A.C., Rossi, M., Reichenbach, P., and
568 Guzzetti, F.: Very-high resolution stereoscopic satellite images for landslide mapping. C. Margottini, P. Canuti,
569 K. Sassa (Eds.), *Landslide Science and Practice, Landslide Inventory and Susceptibility and Hazard Zoning*, 1,
570 Springer, Heidelberg, Berlin, New York, 95–101, https://doi.org/10.1007/978-3-642-31325-7_12, 2013.

571 Ayoub, F., LePrince, S. and Keene, L.: User’s Guide to Cosi-Corr: Co-Registration of Optically Sensed Images
572 and Correlation; California Institute of Technology: Pasadena, CA, USA, pp. 38, 2009.

573 Baldo M., Bicocchi C., Chiocchini U., Giordan D. and Lollino G.: LIDAR monitoring of mass wasting processes:
574 The Radicofani landslide, Province of Siena, Central Italy, *Gemorphology*, 105, 193-201, doi:
575 10.1016/j.geomorph.2008.09.015, 2009.

576 Baiocchi, V., Dominici, D. and Mormile, M.: UAV application in post–seismic environment”, *International*
577 *Archives of the Photogrammetry, Remote Sensing and Spatial Information Sciences*, Volume XL-1/W2, UAV-
578 g2013, 4 – 6 September 2013, Rostock, Germany, pp. 21-25, 2013.

579 Bendea, H., Boccardo, P., Dequal, S., Tondo, G., Marenchino, D. and Piras, M.: Low cost UAV for post-disaster
580 assessment. *Int. Arch. Photogramm. Remote Sens. Spat. Inf. Sci.*, 37, 1373–1379, 2008.

581 Benassai, G., Aucelli, P., Budillon, G., De Stefano, M., Di Luccio, D., Di Paola, G., Montella, R., Mucerino, L.,
582 Sica, M. and Pennetta, M.: Rip current evidence by hydrodynamic simulations, bathymetric surveys and UAV
583 observation. *Nat. Hazards Earth Syst. Sci.*, 17, 1493-1503, <https://doi.org/10.5194/nhess-17-1493-2017>, 2017.

585 Boccardo, P., Chiabrando, F., Dutto, F., Tonolo, F.G. and Lingua, A.: UAV deployment exercise for mapping
586 purposes: Evaluation of emergency response applications, *Sensors*, 15(7), 15717-15737, 2015.

587 Bolognesi, M., Farina, G., Alvisi, S., Franchini, M., Pellegrinelli, A. and Russo, P.: Measurement of surface
588 velocity in open channels using a lightweight remotely piloted aircraft system. *Geomatics, Natural Hazards*
589 and Risk, 8:1, 73.86, 2016. DOI: 10.1080/19475705.2016.1184717

590 Brardinoni, F., Slaymaker, O., and Hassan, M.A.: Landslides inventory in a rugged forested watershed: a
591 comparison between air-photo and field survey data, *Geomorphology*, 54, 179-196,
592 [https://doi.org/10.1016/S0169-555X\(02\)00355-0](https://doi.org/10.1016/S0169-555X(02)00355-0), 2003.

593 Brostow, G.J., Shotton, J., Fauqueur, J. and Cipolla, R.: Segmentation and Recognition Using Structure from
594 Motion Point Clouds. *Proc. 10th European Conf. on Computer Vision: Part I*, 44–57, doi:10.1007/978-3-540-
595 88682-2_5, 2008.

596 Caltabiano, D., Muscato, G., Orlando, A., Federico, C., Giudice, G. and Guerrieri, S.: Architecture of a UAV for
597 volcanic gas sampling, in 2005 IEEE Conference on Emerging Technologies and Factory Automation, 1, 739-
598 744, 2005.

599 Cannioto, M., D'Alessandro, A., Lo Bosco, G., Scudero, S. and Vitale, G.: Brief communication: Vehicle routing
600 problem and UAV application in the post-earthquake scenario, *Nat. Hazards Earth Syst. Sci.*, 17, 1939-
601 1946, <https://doi.org/10.5194/nhess-17-1939-2017>, 2017

602 Carvajal, F., Agüera, F. and Pérez, M.: Surveying a landslide in a road embankment using Unmanned Aerial
603 Vehicle photogrammetry, *ISPRS Arch.*, 38, 1-6, 2011.

604 Casagli N., Frodella, W., Morelli, S., Tofani, V., Ciampalini, A., Intrieri, E., Raspini, F., Rossi, G., Tanteri, L. and
605 Lu, P.: Spaceborne, UAV and ground-based remote sensing techniques for landslide mapping, monitoring and
606 early warning, *Geoenvironmental Disasters*, 4(9), 1-23, DOI 10.1186/s40677-017-0073-1, 2017.

607 Chang, K.J., Chan, Y.C., Chen, R.F. and Hsieh, Y.C.: Geomorphological evolution of landslides near an active
608 normal fault in Northern Taiwan, as revealed by LiDAR and unmanned aircraft system data, *Nat. Hazards
609 Earth Syst. Sci. Discuss.*, <https://doi.org/10.5194/nhess-2017-227>, 2017.

610 Chang-Chun L., Zhang, G., Lei, T. and Gong, A.: Quick image-processing method of UAV without control points
611 data in earthquake disaster area. *Transactions of Nonferrous Metals Society of China*, 21(3), s523-s528, 2011.

612 Chio, S.-H. and Lin, C.-H.: Preliminary Study of UAS Equipped with Thermal Camera for Volcanic Geothermal
613 Monitoring in Taiwan, *Sensors*, 17(7), 1649, doi:10.3390/s17071649, 2017.

614 Costa, D., Burlando, P. and Priadi, C.: The importance of integrated solutions to flooding and water quality
615 problems in the tropical megacity of Jakarta, *Sustain. Cities Soc.*, 20, 199–209, doi:10.1016/j.scs.2015.09.009,
616 2016.

617 Chou, T.Y., Yeh, M.L., Chen, Y. and Chen, Y.H.: Disaster monitoring and management by the unmanned aerial
618 vehicle technology. *Int. Archives of Photogrammetry, Remote Sensing and Spatial Information
619 Sciences*, 38(7B), 137-142, 2010.

620 DeBell, L., Anderson, K., Brazier, R. E., King, N. and Jones, L.: Water resource management at catchment scales
621 using lightweight UAVs: current capabilities and future perspectives, *J. Unmanned Veh. Syst.*, 4(1), 7–30,
622 doi:10.1139/juvs-2015-0026, 2016.

623 Deffontaines, B., Chang, K.J., Champenois, J., Fruneau, B., Pathier, E., Hu, J.C., Lu, S.T. and Liu Y.C.: Active
624 interseismic shallow deformation of the Pingting terraces (Longitudinal Valley – Eastern Taiwan) from UAV
625 high-resolution topographic data combined with InSAR time series. *Geomatics, Natural Hazards and Risk*,
626 8(1), 120-136, 2017.

627 Deffontaines, B., Chang, K.J., Champenois, J., Lin, K.C., Lee, C.T., Chen, R.F, Hu, J.C., and Fruneau, B.: Active
628 tectonics of the onshore Hengchun Fault using UAS DTM combined with ALOS PS-InSAR time series (Southern
629 Taiwan), *Nat. Hazards Earth Syst. Sci. Discuss.*, <https://doi.org/10.5194/nhess-2017-55>, 2017.
630 Delacourt, C., Allemand, P., Jaud, M., Grandjean, P., Deschamps, A., Ammann, J., Cuq, V. and Suanez, S.: DRELIO: An
631 Unmanned Helicopter for Imaging Coastal Areas. *J. Coast. Res.* 56, 1489-1493, 2009.

632 Derrien, A., Villeneuve, N., Peltier, A. and Beauducel, F.: Retrieving 65 years of volcano summit deformation
633 from multitemporal structure from motion: The case of Piton de la Fournaise (La Réunion Island), *Geophys.*
634 *Res. Lett.*, 42(17), 6959–6966, doi:10.1002/2015GL064820, 2015.

635 Deurloo, R., Bastos, L. and Bos, M.: On the Use of UAVs for Strapdown Airborne Gravimetry, pp. 255–261,
636 Springer, Berlin, Heidelberg., 2012.

637 Detzer, S., Weber, M., Touko Tcheumadjeu, L.C., Kuhns, G. and Kendziorra A.: Decision support for
638 multimodal transportation systems at major events and disasters: a case study in the region of Brunswick
639 (Germany). Sener S.M., Brebbia C.A. and Ozcevik O (eds) *Disaster management and Human Health Risk IV*.
640 WIT Press, Southampton, UK, 315-326, 2015.

641 Dewitte, O., J.C. Jasselette, Y. Cornet, M. Van Den Eeckhaut, A. Collignon, J. Poesen, and A. Demoulin.:
642 Tracking landslide displacements by multitemporal DTMs: A combined aerial stereophotogrammetric and
643 LIDAR approach in western Belgium. *Engineering Geology*, 7, 582–586, 2008.

644 Diaz, J. A., Pieri, D., Wright, K., Sorensen, P., Kline-Shoder, R., Arkin, C. R., Fladeland, M., Bland, G.,
645 Buongiorno, M. F., Ramirez, C., Corrales, E., Alan, A., Alegria, O., Diaz, D. and Linick, J.: Unmanned Aerial Mass
646 Spectrometer Systems for In-Situ Volcanic Plume Analysis, *J. Am. Soc. Mass Spectrom.*, 26(2), 292–304,
647 doi:10.1007/s13361-014-1058-x, 2015.

648 Dominici, D., Alicandro, M., Massimi, V.: UAV photogrammetry in the post-earthquake scenario: case studies
649 in L'Aquila. *Geomatics, Natural Hazards and Risk*, 8(1), 87-103, 2017.

650 Dong, L., Shan, J.: A comprehensive review of earthquake-induced building damage detection with remote
651 sensing techniques. *ISPRS Journal of Photogrammetry and Remote Sensing*, 84, pp. 85-99, 2013.

652 Duarte, D., Nex, F., Kerle, N., Vosseman, G.: Towards a more efficient detection of earthquake induced facade
653 damages using oblique UAV imagery. *International Archives of the Photogrammetry, Remote Sensing and*
654 *Spatial Information Sciences*. To be published. 2017.

655 Dunford, R., Michel, K., Gagnage, M., Piégay, H. and Trémelo M.-L.: Potential and constraints of Unmanned
656 Aerial Vehicle technology for the characterization of Mediterranean riparian forest, *International Journal of*
657 *Remote Sensing*, 30, 4915-4935, 2009.

658 Erdelj, M., Król, M. and Natalizio, E.: Wireless Sensor Networks and Multi-UAV systems for natural disaster
659 management, *Comput. Networks*, 124, 72–86, doi:10.1016/j.comnet.2017.05.021, 2017.

660 Eugster, H. and Nebiker, S.: UAV-based augmented monitoring— real-time georeferencing and integration of
661 video imagery with virtual globes. In: *Int. Archives of Photogrammetry, Remote Sensing and Spatial*
662 *Information Sciences*, Beijing, China, 37(B1), 1229–1235. 2008.

663 Ezequiel, C.A.F., Cua, M., Libatiquem, N.C., Tangonan, G.L., Alampay, R., Labuguen, R.T., Favila, C.M.,
664 Honrado, J.L.E., Canos, V., Devaney, C., Loreto, L.B., Bacusmo, J. and Palma, B.: UAV Aerial Imaging

665 Applications for Post-Disaster Assessment, Environmental Management and Infrastructure Development.
666 2014 International Conference on Unmanned Aircraft Systems (ICUAS) Orlando, FL, USA proceedings: 274–
667 283, 2014.

668 Fan, J., Zhang, X., Su, F., Ge, Y., Tarolli, P., Yang, Z., Zeng, C., and Zeng, Z.: Geometrical feature analysis and
669 disaster assessment of the Xinmo landslide based on remote sensing data, *Journal of Mountain Science*, 14,
670 1677–1688, doi:10.1007/s11629-017-4633-3, 2017.

671 Feng, Q., Liu, J. and Gong, J.: Urban Flood Mapping Based on Unmanned Aerial Vehicle Remote Sensing and
672 Random Forest Classifier—A Case of Yuyao, China, *Water*, 7(4), 1437–1455, doi:10.3390/w7041437, 2015.

673 Fernandez Galarreta, J., Kerle, N. and Gerke, M. UAV - based urban structural damage assessment using
674 object - based image analysis and semantic reasoning. *Natural hazards and earth system sciences*, 15(6) pp.
675 1087-1101, 2015.

676 Feurer, D., Planchon, O., El Maaoui, M.A., Boussema, M.R. and Pierrot-Deseilligny, M.: Potential of kite-borne
677 photogrammetry for decimetric and kilometre square 3D mapping: an application for automatic gully
678 detection, *Nat. Hazards Earth Syst. Sci. Discuss.*, <https://doi.org/10.5194/nhess-2017-60>, 2017

679 Fikar, C., Gronalt, M., and Hirsch. P.A.: decision support system for coordinated disaster relief distribution.
680 *Exp. Syst. Appl.* 57, 104–116. doi:10.1016/j.eswa.2016.03.039, 2016.

681 Filizzola, C., Corrado, R., Marchese, F., Mazzeo, G., Paciello, R., Pergola, N. and Tramutoli, V.: RST-FIRES, an
682 exportable algorithm for early-fire detection and monitoring: Description, implementation, and field
683 validation in the case of the MSG-SEVIRI sensor, *Remote Sensing of Environment*, 192, 2-25, 2017.

684 Fiorucci, F., Giordan, D., Santangelo, M., Dutto, F., Rossi, M., and Guzzetti, F.: Criteria for the optimal selection
685 of remote sensing images to map event landslides, *Nat. Hazards Earth Syst. Sci.*, 18, 405-417, 2018.

686 Flener, C., Vaaja, M., Jaakkola, A., Krooks, A., Kaartinen, H., Kukko, A., Kasvi, E., Hyppä, H., Hyppä, J. and
687 Alho, P.: Seamless mapping of river channels at high resolution using mobile LiDAR and UAV-photography,
688 *Remote Sens.*, 5(12), 6382–6407, doi:10.3390/rs5126382, 2013.

689 Fonstad, M.A., Dietrich, J.T., Courville, B.C., Jensen J.L. and Carboneau, P.E.: Topographic structure from
690 motion: a new development in photogrammetric measurement, *Earth Surf. Process. Landforms*, 38, 421-430,
691 2013.

692 Fugazza, D., Scaioni, M., Corti, M., D'Agata, C., Azzoni, R.S., Cernuschi, M., Smiraglia, C. and Diolaiuti, G.A.:
693 Combination of UAV and terrestrial photogrammetry to assess rapid glacier evolution and conditions of
694 glacier hazards, *Nat. Hazards Earth Syst. Sci. Discuss.*, <https://doi.org/10.5194/nhess-2017-198>, 2017.

695 Gerke, M. and Przybilla, H.J.: Accuracy analysis of photogrammetric UAV image blocks: Influence of on-board
696 RTK-GNSS and cross flight patterns, *Photogrammetrie-Fernerkundung-Geoinformation* 2016 (1), 17-30, 2016.

697 Gerke, M. and Kerle, N.: Automatic structural seismic damage assessment with airborne oblique pictometry
698 imagery. In: PE&RS = Photogrammetric Engineering and Remote Sensing, 77(9) pp. 885-898, 2011.

699 Giordan, D., Allasia, P., Manconi, A., Baldo, M., Santangelo, M., Cardinali, M., Corazza, A., Albanese, V.,
700 Lollino, G., and Guzzetti, F.: Morphological and kinematic evolution of a large earthflow: The Montaguto
701 landslide, southern Italy, *Geomorphology*, 187, 61-79, 2013.

702 Giordan, D., Manconi, A., Facello, A., Baldo, M., dell'Anese, F., Allasia, P. and Dutto, F.: Brief Communication
703 "The use of UAV in rock fall emergency scenario", *Nat. Hazards Earth Syst. Sci.*, 15, 163-169, 2015a.

704 Giordan, D., Manconi, A., Tannant, D. and Allasia, P.: UAV: low-cost remote sensing for high-resolution
705 investigation of landslides. *IEEE International Symposium on Geoscience and Remote Sensing IGARSS*, 26-31
706 July 2015, Milan, Italy, 5344-5347, 2015b.

707 Giordan, D., Notti, D., Villa, A., Zucca, F., Calò, F., Pepe, A., Dutto, F., Pari, p., Baldo, M. and Allasia, P.: Low
708 cost, multiscale and multi-sensor application for flooded areas mapping. *Nat. Hazards Earth Syst. Sci.*
709 Discuss. <https://doi.org/10.5194/nhess-2017-420>, 2017

710 Gomez, C.: Digital photogrammetry and GIS-based analysis of the bio-geomorphological evolution of
711 Sakurajima Volcano, diachronic analysis from 1947 to 2006, *J. Volcanol. Geotherm. Res.*, 280, 1-13,
712 doi:10.1016/j.jvolgeores.2014.04.015, 2014.

713 Gomez, C. and Kato, A.: Multi-scale voxel-based algorithm for UAV-derived point-clouds of complex surfaces.
714 *IEEE International ICARES – Aerospace Electronics and Remote Sensing Technology*: 205–209. 2014.

715 Gomez, C. and Purdie, H.: UAV- based Photogrammetry and Geocomputing for Hazards and Disaster Risk
716 Monitoring – A Review. *Geoenvironmental Disasters* 3(23), 1-11, 2016.

717 Gomez, C., Hayakawa, Y. and Obanawa, H.: A study of Japanese landscapes using structure from motion
718 derived DSMs and DEMs based on historical aerial photographs: New opportunities for vegetation monitoring
719 and diachronic geomorphology, *Geomorphology*, 242, 11–20, doi:10.1016/j.geomorph.2015.02.021, 2015.

720 GSI: Information on the 2017 Northern Kyushu Heavy Rain, *Geospatial Inf. Auth. Japan* [online] Available
721 from: http://www.gsi.go.jp/BOUSAII/H29hukuoka_oita-heavyrain.html (Accessed 16 September 2017),
722 2017.

723 Guha-Sapir, D., Hoyois, P., Wallemacq P. and Below, R.: *Annual Disaster Statistical Review 2016 The
724 numbers and trends. Centre for Research on the Epidemiology of Disasters, Ciaco Imprimerie, Louvain-la-
725 Neuve (Belgium)*, pp. 91, 2017.

726 Guzzetti, F., Reichenbach, P., Cardinali, M., Galli, M. and Ardizzone, F.: Probabilistic landslide hazard
727 assessment at the basin scale, *Geomorphology*, 72(1-4), 272-299, 2005.

728 Haneberg, W. C.: Using close range terrestrial digital photogrammetry for 3-D rock slope modeling and
729 discontinuity mapping in the United States, *Bulletin of Engineering Geology and the Environment*, 67(4), 457-
730 469, 2008.

731 Harvey, M. C., Rowland, J. V. and Luketina, K. M.: Drone with thermal infrared camera provides high
732 resolution georeferenced imagery of the Waikite geothermal area, New Zealand, *J. Volcanol. Geotherm. Res.*,
733 325, 61–69, doi:10.1016/j.jvolgeores.2016.06.014, 2016.

734 Hayakawa, Y.S., Yoshida, H., Obanawa, H., Naruhashi, R., Okumura, K., Zaiki, M. and Kontani R.:
735 Characteristics of debris avalanche deposits inferred from source volume estimate and hummock
736 morphology around Mt. Erciyes, central Turkey. *Nat. Hazards Earth Syst. Sci.*, 18, 429-
737 444, <https://doi.org/10.5194/nhess-18-429-2018>, 2018.Hervouet, A., Dunford, R., Piégay, H., Belletti, B. and
738 Trémélo, M.-L.: Analysis of Post-flood Recruitment Patterns in Braided-Channel Rivers at Multiple Scales

739 Based on an Image Series Collected by Unmanned Aerial Vehicles, Ultra-light Aerial Vehicles, and Satellites,
740 *GIScience Remote Sens.*, 48(1), 50–73, doi:10.2747/1548-1603.48.1.50, 2011.

741 Hinkley, E. and Zajkowski, T.: USDA forest service-NASA: unmanned aerial systems demonstrations—pushing
742 the leading edge in fire mapping, *Geocarto Int.*, 26(2), 103-111, 2011.

743 Hirose, M., Xiao, Y., Zuo, Z., Kamat, V. R., Zekkos, D. and Lynch, J.: Implementation of UAV localization
744 methods for a mobile post-earthquake monitoring system, in 2015 IEEE Workshop on Environmental, Energy,
745 and Structural Monitoring Systems (EESMS) Proceedings, pp. 66–71, IEEE., 2015.

746 Huang H., Long J., Lin H., Zang L., Yi W. and Lei B.: Unmanned aerial vehicle based remote sensing method for
747 monitoring a steep mountainous slope in the Three Gorges Reservoir, China, *Earth Science Informatics* 10 (3)
748 287-301, 2017.

749 Huang, H., Long, J., Yi, W., Yi, Q., Zhang, G. and Lei, B.: A method for using unmanned aerial vehicles for
750 emergency investigation of single geo-hazards and sample applications of this method, *Nat. Hazards Earth*
751 *Syst. Sci.*, 17, 1961-1979, <https://doi.org/10.5194/nhess-17-1961-2017>, 2017. Immerzeel, W.W.,
752 Kraaijenbrink, P. D. A., Shea, J. M., Shrestha, A. B., Pellicciotti, F., Bierkens, M. F. P. and de Jonga, S.M.: High-
753 resolution monitoring of Himalayan glacier dynamics using unmanned aerial vehicles, *Remote Sensing of*
754 *Environment*, 150, 93-103, 2014.

755 Izumida, A., Uchiyama, S. and Sugai, T.: Application of UAV-SfM photogrammetry and aerial lidar to a
756 disastrous flood: repeated topographic measurement of a newly formed crevasse splay of the Kinu River,
757 central Japan. *Nat. Hazards Earth Syst. Sci.*, 17, 1505-1519, <https://doi.org/10.5194/nhess-17-1505-2017>, 2017. Jaud, M.; Grasso, F.; Le Dantec, N.; Verney, R.; Delacourt, C.; Ammann, J.; Deloffre, J.; Grandjean,
759 P. Potential of UAVs for Monitoring Mudflat Morphodynamics (Application to the Seine Estuary, France).
760 *ISPRS Int. J. Geo-Inf.* 5(4), 50, 2016.

761 Javernick, L., Brasington, J. and Caruso, B.: Modeling the topography of shallow braided rivers using Structure-
762 from-Motion photogrammetry, *Geomorphology*, 213, 166–182, doi:10.1016/j.geomorph.2014.01.006, 2014.

763 Joyce K. E., Belliss, S. E., Samsonov, S. V., McNeill, S. J. and Glassey, P. J.: A review of the status of satellite
764 remote sensing and image processing techniques for mapping natural hazards and disasters. *Progress in*
765 *Physical Geography*, 33, 83-207, 2009.

766 Kraft, T., Geßner, M., Meißner, H., Cramer, M., Gerke, M. and Przybilla, H.J.: Evaluation of a metric camera
767 system tailored for high precision UAV applications. In: *Proceedings of the XXIII ISPRS Congress : From human*
768 *history to the future with spatial information*, 12-19 July 2016, Prague, Czech Republic. Peer reviewed Annals,
769 Volume III-2, 2016. Comm II, ThS14 recent developments in Open Data - Prague. Vol. XLI-B1, ISSN 2194-9034,
770 2016

771 Klemas, V. V.: Coastal and Environmental Remote Sensing from Unmanned Aerial Vehicles: An Overview,
772 *Journal of Coastal Research*, 31(5), 1260-1267, 2015.

773 Koutsoudisa, A., Vidmarb, B., Ioannakisa, G., Arnaoutoglou, F., Pavlidis, V. and Chamzasc, C.: Multi-image
774 3D reconstruction data evaluation, *Journal of Cultural Heritage*, 15, 73-79, 2014.

775 Lazzari, M. and Gioia D.: UAV images and high-resolution DEMs for geomorphological analysis and hazard
776 evaluation: the case of the Uggiano archaeological site (Ferrandina, southern Italy). *Geomatics, Natural*
777 *Hazards and Risk*, 8(1), 104-119, 2017.

778 Langhammer, J., Lendzioch, T., Miříjovský, J. and Hartvich, F.: UAV-based optical granulometry as tool for
779 detecting changes in structure of flood depositions, *Remote Sens.*, 9(3), doi:10.3390/rs9030240, 2017.

780 Le Coz, J., Patalano, A., Collins, D., Guillén, N. F., García, C. M., Smart, G. M., Bind, J., Chiaverini, A., Le
781 Boursicaud, R., Dramais, G. and Braud, I.: Crowdsourced data for flood hydrology: Feedback from recent
782 citizen science projects in Argentina, France and New Zealand, *J. Hydrol.*, 541, 766–777,
783 doi:10.1016/j.jhydrol.2016.07.036, 2016.

784 Lehmann, F., Berger, R., Brauchle, J. Hein, D., Meißner H. and Pless, S.: MACS - Modular Airborne Camera
785 System for generating photogrammetric high-resolution products. *Zeitschrift der Deutschen Gesellschaft für*
786 *Geowissenschaften*, Schweizerbart Science Publishers, Stuttgart, Germany, (6), pp. 435-446, 2011

787 Leprince, S., Berthier, E., Ayoub, F., Delacourt, C. and Avouac, J.-P.: Monitoring Earth Surface Dynamics With
788 Optical Imagery, *Eos, Trans. Am. Geophys. Union*, 89(1), 1–2, doi:10.1029/2008EO010001, 2008.

789 Leprince, S., Barbot, S., Ayoub, F. and Ayouac, J.P.: Automatic and precise orthorectification, co-registration,
790 and sub-pixel correlation of satellite images, application to ground deformation measurements. *IEEE Trans.*
791 *Geosci. Remote Sens.* 46, 1529-1558, 2007.

792 Li, Y., Gong, J. H., Zhu, J., Ye, L., Song, Y. Q. and Yue, Y. J.: Efficient dam break flood simulation methods for
793 developing a preliminary evacuation plan after the Wenchuan Earthquake, *Nat. Hazards Earth Syst. Sci.*,
794 12(1), 97–106, doi:10.5194/nhess-12-97-2012, 2012.

795 Lindner, G., Schraml, K., Mansberger, R. and Hubl J.: UAV monitoring and documentation of a large landslide.
796 *Appl Geomat*, 8(1), 1-11, 2016.

797 Liu, C.-C., Chen, P.-L., Tomoya, M., Chen, C.-Y.: Rapidly responding to landslides and debris flow events using
798 a low-cost unmanned aerial vehicle. *J. Rem. Sens.* 9(1), 1-11, doi:10.1111/1.JRS.9.096016, 2015.

799 Lucieer, A., de Jong S. M. and Turner, D.: Mapping landslide displacements using Structure from Motion (SfM)
800 and image correlation of multi-temporal UAV photography, *Progress in Physical Geography*, 38(1), 97–116,
801 2014a.

802 Lucieer, A., Turner, D., King, D. H. and Robinson, S. A.: Using an Unmanned Aerial Vehicle (UAV) to capture
803 microtopography of Antarctic moss beds. *International Journal of Applied Earth Observation and*
804 *Geoinformation*. 27(a), 53–62, 2014b.

805 Manferdini, A.M.: A Methodology for the Promotion of Cultural Heritage Sites Through the Use of Low-Cost
806 Technologies and Procedures. In: proc. 17th Int. Conf. on 3D Web Technology Los Angeles, CA, August 4-5,
807 2012, 180, 2012.

808 Martin, P. G., Smith, N. T., Yamashiki, Y., Payton, O. D., Russell-Pavier F. S., Fardoulis, J. S., Richards D. A. and
809 Scott T. B.: 3D unmanned aerial vehicle radiation mapping for assessing contaminant distribution and
810 mobility, *International Journal of Applied Earth Observation and Geoinformation*, 52, 12-19, 2016.

811 Marek, L., Miříjovský, J. and Tuček, P.: Monitoring of the Shallow Landslide Using UAV Photogrammetry and
812 Geodetic Measurements, In: Lollino G., Giordan D., Crosta G.B., Corominas J., Azzam R. Wasowski J., Sciarra
813 N. (eds.) *Engineering Geology for Society and Territory – Landslide Processes*, Springer International
814 Publishing Switzerland, 2, 113-116, 2015.

815 Martinez-de Dios, J.R., Merino, L., Caballero, F. and Ollero, A.: Automatic forest-fire measuring using ground
816 stations and unmanned aerial systems. *Sensors*, 11(6), 6328-6353, 2011.

817 McKenzie, D., Shankar, U., Keane, R. E., Stavros, E. N., Heilman, W. E., Fox, D. G. and Riebau, A. C.: Smoke
818 consequences of new wildfire regimes driven by climate change, *Earth's Future*, 2(2), 35-59, 2014.

819 Merino, L., Caballero, F., Martínez-de-Dios, J.R., Iván, M. and Aníbal, O.: An unmanned aircraft system for
820 automatic forest fire monitoring and measurement, *J. Intell. Rob. Syst.*, 65(1-4), 533-548, 2012.

821 McGonigle, A. J. S., Aiuppa, A., Giudice, G., Tamburello, G., Hodson, A. J. and Gurrieri, S.: Unmanned aerial
822 vehicle measurements of volcanic carbon dioxide fluxes, *Geophys. Res. Lett.*, 35(6), 3-6,
823 doi:10.1029/2007GL032508, 2008.

824 Middlemiss, R.P., Samarelli, A., Paul, D.J., Hough, J., Rowan, S. and Hammond, G.D.: The First Measurement
825 of the Earth Tides with a MEMS Gravimeter, *Nature*, 531(1), 614, 2016.

826 Molina, P., Colomina, I., Vitoria, T., Silva, P.F., Skaloud, J., Kornus, W., Prades, R. and Aguilera, C.: Searching
827 lost people with UAVs: the system and results of the close-search project. *International Archives of the
828 Photogrammetry, Remote Sensing and Spatial Information Sciences*, 39(B1), 441-446, 2012.

829 Mori, T., Hashimoto, T., Terada, A., Yoshimoto, M., Kazahaya, R., Shinohara, H. and Tanaka, R.: Volcanic plume
830 measurements using a UAV for the 2014 Mt. Ontake eruption, *Earth, Planets Sp.*, 68(1), 49,
831 doi:10.1186/s40623-016-0418-0, 2016.

832 Murphy, R. R., Steimle, E., Griffin, C., Cullins, C., Hall, M. and Pratt, K.: Cooperative use of unmanned sea
833 surface and micro aerial vehicles at Hurricane Wilma, *Journal of Field Robotics*, 25(3), 164-180, 2008.

834 Nakamura, F., Shimatani, Y., Nishihiro, J., Ohtsuki, K., Itsukushima, R. and Yamada, H.: Report on flood
835 disaster in Kinu River, occurred in September, 2015 (in Japanese with English abstract), *Ecol. Civ. Eng.*, 19(2),
836 259-267, doi:10.3825/ece.19.259, 2017.

837 Nagatani, K., Akiyama, K., Yamauchi, G., Otsuka, H., Nakamura, T., Kiribayashi, S., Yoshida, K., Hada, Y., Yuta,
838 S., Fujino, K., Izu, T. and Mackay, R.: Volcanic ash observation in active volcano areas using teleoperated
839 mobile robots - Introduction to our robotic-volcano-observation project and field experiments, in: proc. 2013
840 IEEE International Symposium on Safety, Security, and Rescue Robotics (SSRR), Linkoping, Sweden, 21-26 Oct.
841 2013, 1-6, 2013.

842 Nakano, T., Kamiya, I., Tobita, M., Iwahashi, J. and Nakajima, H.: Landform monitoring in active volcano by
843 UAV and SFM-MVS technique, *Int. Arch. Photogramm. Remote Sens. Spat. Inf. Sci. - ISPRS Arch.*, 40(8), 71-
844 75, 2014.

845 Nedjati, A., Vizvari, B., Izbirak, G.: Post-earthquake response by small UAV helicopters, *Nat. Hazards* 80, 1669-
846 1688, 2016. Doi: <http://dx.doi.org/10.1007/s11069-015-2046-6>

847 Nex, F., Gerke, M., Remondino, F., Przybilla H.-J., Bäumker, M. and Zurhorst, A.: ISPRS Benchmark for Multi-
848 Platform Photogrammetry. *ISPRS Annals of the Photogrammetry, Remote Sensing and Spatial Information
849 Sciences*, Vol. II3/W4, 135-142, 2015.

850 Nex, F. and Remondino, F.: UAV for 3D mapping applications: a review, *Appl. Geomatics*, 6(1), 1-15,
851 doi:10.1007/s12518-013-0120-x, 2014.

852 Nex, F., Rupnik, E., Toschi, I., Remondino, F. Automated processing of high resolution airborne images for
853 earthquake damage assessment. In: International Archives of Photogrammetry and Remote Sensing and
854 Spatial Information Sciences, Vol. XL-1, 2014

855 Niculită, M.: Automatic landslide length and width estimation based on the geometric processing of the
856 bounding box and the geomorphometric analysis of DEMs, *Nat. Hazards Earth Syst. Sci.*, 16, 2021-2030,
857 <https://doi.org/10.5194/nhess-16-2021-2016>, 2016.

858 Niethammer, U., James, M.R., Rothmund, S., Travelletti, J. and Joswig, M.: UAV-based remote sensing of the
859 Super-Sauze landslide: evaluation and results, *Eng Geol.*, 128, 2-11, 2012.

860 Niethammer, U., Rothmund, S., James, M.R., Travelletti, J. and Joswig, M.: UAV-based remote sensing of
861 landslides. In *Proceedings of the International Archives of Photogrammetry, Remote Sensing and Spatial*
862 *Information Sciences, Commission V Symposium, Newcastle upon Tyne, UK, 21–24 June 2010*, 496–501,
863 2010.

864 Niethammer, U., Rothmund, S., Joswig, M.: UAV-based remote sensing of the slow-moving landslide Super-
865 Sauze. In: Malet, J.-P., Remaître, A., Boogard, T. (Eds) *Proceedings of the International Conference on*
866 *Landslide Processes: from geomorphologic mapping to dynamic modelling*, Strasbourg, CERG Editions, pp. 69-
867 74, 2009.

868 Niethammer, U., Rothmund, S., Schwaderer, U., Zeman, J., Joswig, M.: Open Source Image-Processing Tools
869 for Low-Cost UAV-Based Landslide Investigations. *International Archives of the Photogrammetry, Remote*
870 *Sensing and Spatial Information Sciences, Volume XXXVIII-1/C22, 2011 ISPRS Zurich 2011 Workshop*, 14-16
871 September 2011, Zurich, Switzerland, 161-166, 2011.

872 Nishar, A., Richards, S., Breen, D., Robertson, J. and Breen, B.: Thermal infrared imaging of geothermal
873 environments and by an unmanned aerial vehicle (UAV): A case study of the Wairakei - Tauhara geothermal
874 field, Taupo, New Zealand, *Renew. Energy*, 86, 1256–1264, doi:10.1016/j.renene.2015.09.042, 2016.

875 Nocerino, E., Menna, F., Remondino, F. and Saleri, R: Accuracy and block deformation analysis in automatic
876 UAV and terrestrial photogrammetry - Lesson learnt. *ISPRS Annals of the Photogrammetry, Remote Sensing*
877 *and Spatial Information Sciences, Vol. II(5/W1), Proc. 24th Intern. CIPA Symposium, 2–6 Sept., Strasbourg,*
878 *France. pp. 203-208.* 2013

879 Obanawa, H., Y. Hayakawa, and C. Gomez.: 3D Modelling of inaccessible Areas using UAV-based Aerial
880 Photography and Structure from Motion. *Transactions of the Japanese Geomorphological Union*, 35, 283–
881 294. 2014.

882 Peppa, M.V., Mills, J.P., Moore, P. Miller, P.E. and Chambers, J.E.: Brief communication: Landslide motion
883 from cross correlation of UAV-derived morphological attributes. *Nat. Hazards Earth Syst. Sci.*, 17, 2143-
884 2150, <https://doi.org/10.5194/nhess-17-2143-2017>, 2017

885 Peters, M. P., Iverson, L. R., Matthews, S. N. and Prasad, A. M.: Wildfire hazard mapping: exploring site
886 conditions in eastern US wildland–urban interfaces, *International Journal of Wildland Fire*, 22, 567-578, 2013.

887 Pham, T.-T.-H., P. Apparicio, C. Gomez, C. Weber, and D. Mathon.: Towards a rapid automatic detection of
888 building damage using remote sensing for disaster management. *The Haiti earthquake. Dis. Prev. Manage*,
889 23, 53–66, 2014. doi: 10.1108/DPM-12-2012-0148

890 Piras, M., Taddia, G., Forno, M.G., Gattiglio, M., Aicardi, I., Dabove, P., Lo Russo, S. and Lingua, A.: Detailed
891 geological mapping in mountain areas using an unmanned aerial vehicle: application to the Rodoretto Valley,
892 NW Italian Alps, *Geomatics, Natural Hazards and Risk*, 8(1), 137-149, 2017.

893 Pollefey, M., Gool, L. V., Vergauwen, M., Cornelis, K., Verbiest, F. and Tops, J.: Image-Based 3D Acquisition
894 of Archaeological Heritage and Applications. *Proc. Conf. on Virtual Reality, Archeology, and Cultural Heritage*,
895 255–262, 2001.

896 Pratt, K.S., Murphy, R., Stover, S. and Griffin, C.: Conops and autonomy recommendations for VTOL small
897 unmanned aerial system based on Hurricane Katrina operations, *Journal of Field Robotics*, 26(8), 636-650,
898 2009.

899 Pyo, J., Cho, H., Joe, H., Ura, T. and Yu, S.: Development of hovering type AUV “ Cyclops ” and its performance
900 evaluation using image mosaicing, *Ocean Eng.*, 109, 517–530, doi:10.1016/j.oceaneng.2015.09.023, 2015.

901 Rau, J.Y., Jhan, J.P., Lo, C.F. and Lin Y. S.: Landslide mapping using imagery acquired by a fixed-wing UAV,
902 International Archives of the Photogrammetry, Remote Sensing and Spatial Information Sciences, Volume
903 XXXVIII-1/C22, 2011 ISPRS Zurich 2011 Workshop, 14-16 September 2011, Zurich, Switzerland, 195-200,
904 2011.

905 Razak, K. A., Santangelo, M., Van Westen, C. J., Straatsma, M. W., and de Jong, S. M.: Generating an optimal
906 DTM from airborne laser scanning data for landslide mapping in a tropical forest environment,
907 *Geomorphology*, 190, 112-125, 25 <https://doi.org/10.1016/j.geomorph.2013.02.021>, 2013

908 Rossi, G., Tanteri, L., Tofani, V., Vannucci, P., Moretti, S., and Casagli, N.: Brief Communication: Use of
909 multicopter drone optical images for landslide mapping and characterization, *Nat. Hazards Earth Syst. Sci.*
910 Discuss., <https://doi.org/10.5194/nhess-2017-46>, 2017

911 Ryan, J. C., Hubbard, A. L., Box, J. E., Todd, J., Christoffersen, P., Carr, J. R., Holt, T. O., and Snooke, N.: Repeat
912 UAV photogrammetry to assess calving front dynamics at a large outlet glacier draining the Greenland Ice
913 Sheet, *The Cryosphere*, 9, 1-11, 2015.

914 Saiki, K. and Ohba, T.: Development of an unmanned observation aerial vehicle (UAV) as a tool for volcano
915 survey (in Japanese with English abstract), *Bull. Volcanol. Soc. Japan Second Ser.*, 55(3), 137–146, 2010.

916 Salvini, R., Mastrorocco, G., Seddaiu, M., Rossi, D. and Vanneschi, C.: The use of an unmanned aerial vehicle
917 for fracture mapping within a marble quarry (Carrara, Italy): photogrammetry and discrete fracture network
918 modelling, *Geomatics, Natural Hazards and Risk*, 8(1), 34-52, 2017.

919 Salvini, R., Mastrorocco, G., Esposito, G., Di Bartolo, S., Coggan, J. and Vanneschi, C.: Use of a remotely piloted
920 aircraft system for hazard assessment in a rocky mining area (Lucca, Italy). *Nat. Hazards Earth Syst. Sci.*, 18,
921 287-302, <https://doi.org/10.5194/nhess-18-287-2018>, 2018Sanada, Y. and Torii T.: Aerial radiation
922 monitoring around the Fukushima Dai-ichi nuclear power plant using an unmanned helicopter, *Journal of
923 Environmental Radioactivity*, 139, 294-299, 2015.

924 Santangelo, M., Cardinali, M., Rossi, M., Mondini, A. C., and Guzzetti, F.: Remote landslide mapping using a
925 laser rangefinder binocular and GPS, *Nat. Hazards Earth Syst. Sci.*, 10, 2539-2546, doi:10.5194/nhess-10-
926 2539-2010, 2010.

927 Saroglou, C., Asteriou, P., Zekkos, D., Tsiambaos, G., Clark, M., and Manousakis, J.: UAV-enabled
928 reconnaissance and trajectory modeling of a co-seismic rockfall in Lefkada, *Nat. Hazards Earth Syst. Sci.*, 18,
929 321-333, <https://doi.org/10.5194/nhess-18-321-2018>, 2018.

930 Scaioni, M., Longoni, L., Melillo, V. and Papini, M.: Remote Sensing for Landslide Investigations: An Overview
931 of Recent Achievements and Perspectives, *Remote Sens.* 6(10), 9600-9652, 2014,

932 Schroeder, W., Oliva, P., Giglio, L., Quayle, B., Lorenz, E. and Morelli, F.: Active fire detection using Landsat-
933 8/OLI data, *Remote Sensing of Environment*, 185, 210-220, 2016.

934 Șerban, G., Rus, I., Vele, D., Brețcan, P., Alexe, M. and Petrea, D.: Flood-prone area delimitation using UAV
935 technology, in the areas hard-to-reach for classic aircrafts: case study in the north-east of Apuseni Mountains,
936 Transylvania, *Nat. Hazards*, 82(3), 1817–1832, doi:10.1007/s11069-016-2266-4, 2016.

937 Shinohara, H.: Composition of volcanic gases emitted during repeating Vulcanian eruption stage of
938 Shinmoedake, Kirishima volcano, Japan, *Earth Planets Sp.*, 65(6), 667–675, doi:10.5047/eps.2012.11.001,
939 2013.

940 Smith, M. W., Carrivick, J. L., Hooke, J. and Kirkby, M. J.: Reconstructing flash flood magnitudes using
941 “Structure-from-Motion”: A rapid assessment tool, *J. Hydrol.*, 519, 1914–1927,
942 doi:10.1016/j.jhydrol.2014.09.078, 2014.

943 Sohn, H., Heo, J., Yoo, H., Kim, S. and Cho, H.: Hierarchical multi-sensor approach for the assessment of flood
944 related damages, *Proc. XXI Congr.*, 207–210, 2008.

945 Stöcker, C., Bennett, R., Nex, F., Gerke, M. and Zevenbergen, J.: Review of the current state of UAV
946 regulations, *Remote Sensing* 9(5), 459, doi:10.3390/rs9050459, 2017.

947 Tang, L. and Shao, G.: Drone remote sensing for forestry research and practices. *J. For. Res.*, 26, 791-797,
948 2015.

949 Thamm, H.P. and Judex, M.: The “Low cost drone” – An interesting tool for process monitoring in a high
950 spatial and temporal resolution. *The International Archives of Photogrammetry, Remote Sensing and Spatial
951 Information Sciences*, Enschede, The Netherlands, Vol. XXXVI part 7. 2006

952 Tamminga, A. D., Eaton, B. C. and Hugenholtz, C. H.: UAS-based remote sensing of fluvial change following
953 an extreme flood event, *Earth Surf. Process. Landforms*, 40(11), 1464–1476, doi:10.1002/esp.3728, 2015.

954 Tannant, D. D., Giordan, D. and Morgenroth J.: Characterization and analysis of a translational rockslide on a
955 stepped-planar slip surface. *Engineering Geology*, 220, 144-151, 2017.

956 Tarolli, P.: High-resolution topography for understanding Earth surface processes: opportunities and
957 challenges, *Geomorphology*, 216, 295–312, 2014.

958 Tobita, M., Kamiya, I., Iwahashi, J., Nakano, T. and Takakuwa, N.: UAV aerial photogrammetry in Nishinoshima
959 Island and its analysis (in Japanese), *Bull. Geospatial Inf. Auth. Japan*, 125, 115–124, 2014a.

960 Tobita, M., Kamiya, I., Nakano, T., Iwahashi, J., Osumi, K. and Takakuwa, N.: Precise UAV aerial
961 photogrammetry in Nishinoshima Island (in Japanese), *Bull. Geospatial Inf. Auth. Japan*, 125, 145–154, 2014b.

962 Tokarczyk, P., Leitao, J. P., Rieckermann, J., Schindler, K. and Blumensaat, F.: High-quality observation of
963 surface imperviousness for urban runoff modelling using UAV imagery, *Hydrol. Earth Syst. Sci.*, 19(10), 4215–
964 4228, doi:10.5194/hess-19-4215-2015, 2015.

965 Torrero, L. Seoli, L. Molino, A. Giordan, D. Manconi, A. Allasia, P. and Baldo, M.: The Use of Micro-UAV to
966 Monitor Active Landslide Scenarios, in: *Engineering Geology for Society and Territory*, edited by: Lollino, G.,
967 Manconi, A., Guzzetti, F., Culshaw, M., Bobrowsky P., and Luino, F., Springer International Publishing
968 Switzerland, 5, 701-704, doi:10.1007/978-3-319-09048-1_136, 2015.

969 Török, Á., Barsi, Á., Bögöly, G., Lovas, T., Somogyi, Á., and Görög, P.: Slope stability and rock fall hazard
970 assessment of volcanic tuffs using RPAS and TLS with 2D FEM slope modelling, *Nat. Hazards Earth Syst. Sci.*,
971 18, 583-597, 2018.

972 Travelletti, J., Delacourt, C., Allemand, P., Malet, J.P., Schmittbuhl, J., Toussaint, R. and Bastard, M.:
973 Correlation of multi-temporal ground-based optical images for landslide monitoring: application, potential
974 and limitations, *ISPRS J Photogramm Remote Sens*, 70, 39-55, 2012.

975 Tu, J., Sui, H., Feng, W., Sun, K., Xu, C. and Han, Q.: Detecting building facade damage from oblique aerial
976 images using local symmetry feature and the Gini Index. *Remote Sensing Letters*, 8(7), 676-685, 2017.

977 Turner, D. and Lucieer, A.: Using a micro unmanned aerial vehicle (UAV) for ultra-high resolution mapping
978 and monitoring of landslide dynamics. In *Proceedings of the IEEE International Geoscience and Remote
979 Sensing Symposium*, Melbourne, Australia, 25 July 2013.

980 Turner, D., Lucieer, A. and Watson, C.: An automated technique for generating georectified mosaics from
981 ultrahigh resolution unmanned aerial vehicle (UAV) imagery, structure from motion (SfM) point
982 clouds. *Remote Sens.*, 4(12), 1392-1410, 2012.

983 Turner, D., Lucieer, A. and de Jong, S.M.: Time Series Analysis of Landslide Dynamics Using an Unmanned
984 Aerial Vehicle (UAV), *Remote Sensing*, 7(2), 1736-1757, 2015.

985 UVS international: <https://uvs-international.org>, last access 3 March 2018.

986 Van Den Eeckhaut, M., Poesen, J., Verstraeten, G., Vanacker, V., Nyssen, J., Moeyersons, J., van Beek, L. P. H.,
987 and Vandekerckhove, L.: Use of LIDAR-derived images for mapping old landslides under forest, *Earth Surf.
988 Proc. Land.*, 32, 754-769, <https://doi.org/10.1002/esp.1417>, 2007.

989 Van Westen J.C., Castellanos, E. and Kuriakose S.L.: Spatial data for landslide susceptibility, hazard, and
990 vulnerability assessment: An overview. *Engineering Geology*, 102(3–4), 112-131, 2008.

991 Vetrivel, A., Gerke, M., Kerle, N., Nex, F. and Vosselman, G.: Disaster damage detection through synergistic
992 use of deep learning and 3D point cloud features derived from very high resolution oblique aerial images,
993 and multiple-kernel-learning. *ISPRS Journal of Photogrammetry and Remote Sensing*, doi:
994 10.1016/j.isprsjprs.2017.03.001, in press.

995 Vetrivel, A., Gerke, M., Kerle, N. and Vosselman, G.: Identification of damage in buildings based on gaps in
996 3D point clouds from very high resolution oblique airborne images. *ISPRS Journal of Photogrammetry and
997 Remote Sensing*, 105, 61-78, 2015.

998 Walter, M., Niethammer, U., Rothmund, S. and Joswig, M.: Joint analysis of the Super-Sauze (French Alps)
999 mudslide by nanoseismic monitoring and UAV-based remote sensing. *EAGE First Break*, 27(8), 75-82, 2009.

1000 Wen, Q., He, H., Wang, X., Wu, W., Wang, L., Xu, F., Wang, P., Tang, T. and Lei, Y.: UAV remote sensing hazard
1001 assessment in Zhouqu debris flow disaster, in: *Remote Sensing of the Ocean, Sea Ice, Coastal Waters, and*
1002 *Large Water Regions*, Bostater, C.R., Ertikas, S.P., Neyt X. and Velez-Reyes, M. (eds.), , 8 pp., 2011.

1003 Westoby, M. J., Brasington, J., Glasser, N. F., Hambrey, M. J. and Reynolds, M. J.: Structure-from-Motion
1004 photogrammetry: A low-cost, effective tool for geoscience applications. *Geomorphology*, 179, 300-314,
1005 2012.

1006 Wing, M. G., Burnett J. D. and Sessions, J.: Remote sensing and unmanned aerial system technology for
1007 monitoring and quantifying forest fire impacts, *Int J Remote Sens Appl.*, 4(1), 18-35, 2014.

1008 Witek, M., Jeziorska, J. and Niedzielski, T.: An experimental approach to verifying prognoses of floods using
1009 an unmanned aerial vehicle, *Meteorol. Hydrol. Water Manag.*, 2(1), 3-11 [online] Available from:
1010 <http://www.mhwm.pl/An-experimenta-lapproach-to-verifying-prognoses-of-floods-using-unmanned-aerial-vehicle,0,8.html>, 2014.

1012 Woodget, A. S., Carbonneau, P. E., Visser, F. and Maddock, I. P.: Quantifying submerged fluvial topography
1013 using hyperspatial resolution UAS imagery and structure from motion photogrammetry, *Earth Surf. Process.
1014 Landforms*, 40, 47-64, doi:10.1002/esp.3613, 2015.

1015 Yajima, R., Nagatani, K. and Yoshida, K.: Development and field testing of UAV-based sampling devices for
1016 obtaining volcanic products, in *2014 IEEE International Symposium on Safety, Security, and Rescue Robotics*,
1017 27-30 Oct. 2014, Hokkaido, Japan, 1-5, 2014.

1018 Xie, Z., J. Yang, C. Peng, Y. Wu, X. Jiang, R. Li, Y. Zheng, Y. Gao, S. Liu, and B. Tian.: Development of an UAS for
1019 post-earthquake disaster surveying and its application in Ms7.0 Lushan Earthquake, Sichuan, China. *Comput.
1020 Geosc.* 68, 22-30, 2014.

1021 Yoon, W.S., Jeong, U.J. and Kim, J.H.: Kinematic analysis for sliding failure of multi-faced rock slopes,
1022 *Engineering Geology*, 67, 51-61, 2002.

1023 Zajkowski, T.J., Dickinson, M.B., Hiers, J.K., Holley, W., Williams, B.W., Paxton, A., Martinez, O. and Walker,
1024 G.W.: Evaluation and use of remotely piloted aircraft systems for operations and research – RxCADRE 2012.
1025 *International Journal of Wildland Fire*, 25, 114-128, 2015.

1026 Zazo, S., Molina, J. L. and Rodríguez-Gonzálvez, P.: Analysis of flood modeling through innovative geomatic
1027 methods, *J. Hydrol.*, 524, 522-537, doi:10.1016/j.jhydrol.2015.03.011, 2015.